

Document downloaded from:

<http://hdl.handle.net/10251/153378>

This paper must be cited as:

Lindblad, P.; Fuente-Herraiz, D.; Borbe, F.; Cicchi, B.; Conejero, JA.; Couto, N.; Celesnik, H.... (2019). CyanoFactory, a European consortium to develop technologies needed to advance cyanobacteria as chassis for production of chemicals and fuels. *Algal Research*. 41:1-15. <https://doi.org/10.1016/j.algal.2019.101510>



The final publication is available at

<https://doi.org/10.1016/j.algal.2019.101510>

Copyright Elsevier

Additional Information

Manuscript Details

| | |
|--------------------------|--|
| Manuscript number | ALGAL_2018_1086 |
| Title | CyanoFactory, a European consortium to develop technologies needed to advance cyanobacteria as photoautotrophic production chassis |
| Article type | Full Length Article |

Abstract

CyanoFactory, Design, construction and demonstration of solar biofuel production using novel (photo)synthetic cell factories, was an R&D project developed in response to the FP7-ENERGY- 2012-1 call “Future Emerging Technologies” and the need for significant advances in both new science and technologies to convert solar energy into fuel. CyanoFactory was an example of “purpose driven” research and development with identified scientific goals which also creates a new basic technology. The present overview highlights significant outcomes of the project three years after its successful completion. The scientific progress of CyanoFactory involved the: (i) Development of a ToolBox for cyanobacterial synthetic biology, (ii) Construction of DataWarehouse/Bioinformatics web-based capacities and functions, (iii) Improvement of chassis growth, functionality and robustness, (iv) Introduction of custom designed genetic constructs into cyanobacteria, (v) Improvement of photosynthetic efficiency towards hydrogen production, (vi) Biosafety mechanisms, (vii) Analyses of the designed cyanobacterial cells to identify bottlenecks with suggestions on further improvements, (viii) Metabolic modelling of engineered cells, (ix) Development of an efficient laboratory scale photobioreactor unit, and (x) the Assembly and experimental performance assessment of a larger (1350 L) outdoor flat panel photobioreactor system during two seasons. CyanoFactory - Custom design and purpose construction of microbial cells for the production of desired products using synthetic biology – aimed to go beyond conventional paths to pursue innovative and high impact goals. CyanoFactory brought together ten leading European partners (universities, research organizations and enterprises) with the common goal of developing the future technologies Synthetic biology and Advanced photobioreactors. A provisional patent application and subsequently a European Patent Request were submitted covering construction and methods for the production of target molecules in a cyanobacterium. From societal perspective, the article Making-of Synthetic Biology: The European CyanoFactory Research Consortium (Wünschiers, 2016) was a contribution towards the discussion about synthetic biology and its impact on our society.

| | |
|---|---|
| Keywords | Cyanobacterial synthetic biology toolbox; DataWarehouse; Chassis robustness; Biosafety; Improved electron chain; Large-scale photobioreactor cultivation |
| Taxonomy | Biocatalyst Preparation, Biotechnology, Biosafety, Synthetic Biology, Genetic Engineering, Bioinformatics |
| Manuscript category | Algal Biotechnology |
| Corresponding Author | Peter Lindblad |
| Corresponding Author's Institution | Chemistry-Ångström |
| Order of Authors | Peter Lindblad, David Fuente, Friederike Borbe, Bernardo Cicchi, J. Alberto Conejero, Narciso Couto, Helena Celesnik, Marcello Diano, Marko Dolinar, Serena Esposito, Caroline Evans, Eunice Ferreira, Joseph Keller, Namita Khanna, Gabriel Kind, Andrew Landels, Lenin Lemus, Josselin Noirel, Sarah Ocklenburg, Paulo Oliveira, Catarina Pacheco, Jennifer Parker, Jose Pereira, Khoa Pham, Filipe Pinto, Sascha Rexroth, Matthias Rögner, Hans-Jurgen Schmitz, Ana Margarita Silva Benavides, Maria Siurana, Paula Tamagnini, Eleferios Touloupakis, Giuseppe Torzillo, Javier Urchueguía, Adam Wegelius, Katrin Wiegand, Phillip Wright, Mathias Wutschel, Röbbie Wünschiers |
| Suggested reviewers | Olaf Kruse, Xiang Gao, Tadashi Matsunaga, Koji Sode |

Submission Files Included in this PDF

File Name [File Type]

CyanoFactory - Cover letter.doc [Cover Letter]

CyanoFactory - Highlights.docx [Highlights]

CyanoFactory ms.docx [Manuscript File]

Figures, All.docx [Figure]

Tables.docx [Table]

CyanoFactory - Conflict_of_Interest.docx [Conflict of Interest]

To view all the submission files, including those not included in the PDF, click on the manuscript title on your EVISE Homepage, then click 'Download zip file'.

Research Data Related to this Submission

There are no linked research data sets for this submission. The following reason is given:
Data will be made available on request

Dear Dr. Olivares, Editor-in-Chief of *Algal Research*,

Please find submitted a novel manuscript entitled “CyanoFactory, a European consortium to develop technologies needed to advance cyanobacteria as photoautotrophic production chassis” for consideration by *Algal Research*.

This work summarises the knowledge gained during this European project in the field of algal biotechnology. This research was carried out by 10 teams working together to develop breakthrough technologies to close the gap between actual scientific knowledge and the future biotechnological industry, which will employ photosynthetic microorganisms to produce high-value compounds, such as hydrogen. As consortium, we decided to make this summary three years after the completion of the project.

Some of the most relevant advances achieved within our consortium include novel promoters and other synthetic biology parts for enhanced transcription and translation within cyanobacterial applications, robust and biosafe chassis, improved electron flow towards hydrogen production or cultivation of large-scale outdoor photobioreactor for producing relevant metabolites under solar light.

All authors approved the manuscript and its submission to the journal. We confirm that this work is original and has not been published elsewhere nor is it currently under consideration for publication elsewhere.

Thank you for your consideration of this manuscript.

Sincerely,

/Peter Lindblad, corresponding author

Highlights

- Novel synthetic biology parts for expression of proteins in cyanobacteria developed
- New genomic neutral sites in *Synechocystis* 6803 chromosome discovered and target genes for improved chassis robustness identified
- Rationally designed FNR constructs with increased electron flow towards the hydrogenase enzyme developed
- Proteomic assessment of *Synechocystis* 6803 and mutants performed
- An innovative large-scale flat-panel PBR system designed and experimentally tested

1
2
3
4 **1 CyanoFactory, a European consortium to develop technologies needed to advance**
5 **2 cyanobacteria as photoautotrophic production chassis**
6
7
8
9
10
11
12
13
14
15
16
17
18
19
20
21
22
23
24
25
26
27
28
29
30
31
32
33
34
35
36
37
38
39
40
41
42
43
44
45
51
52
53
54
55
56
57
58
59
60

Peter Lindblad¹, David Fuente¹³, Friederike Borbe¹⁵, Bernardo Cicchi¹⁶, J. Alberto Conejero¹⁴, Narciso Couto⁹, Helena Čelešnik⁸, Marcello M. Diano¹⁸, Marko Dolinar⁸, Serena Esposito¹⁸, Caroline Evans⁹, Eunice A. Ferreira^{3,4,6}, Joseph Keller⁷, Namita Khanna¹, Gabriel Kind², Andrew Landels^{9,10}, Lenin Lemus¹³, Josselin Noirel¹², Sarah Ocklenburg¹⁵, Paulo Oliveira^{3,4}, Catarina C. Pacheco^{3,4}, Jennifer L. Parker⁹, José Pereira^{3,4}, T. Khoa Pham⁹, Filipe Pinto^{3,4}, Sascha Rexroth⁷, Matthias Rögner⁷, Hans-Jürgen Schmitz¹⁵, Ana Margarita Silva Benavides^{16,17}, Maria Siurana¹⁴, Paula Tamagnini^{3,4,5}, Elefterios Touloupakis¹⁶, Giuseppe Torzillo¹⁶, Javier F. Urchueguía¹³, Adam Wegelius¹, Katrin Wiegand⁷, Phillip C. Wright^{9,11}, Mathias Wutschel¹⁵, Röbbbe Wünschiers²

¹ Microbial chemistry, Department of Chemistry – Ångström, Uppsala University, Box 523, SE-751 20 Uppsala, Sweden

² Biotechnology and Chemistry, University of Applied Sciences, Technikumplatz 17, DE-09648 Mittweida, Germany

³ i3S – Instituto de Investigação e Inovação em Saúde, Universidade do Porto, Portugal

⁴ IBMC- Instituto de Biologia Molecular e Celular, Universidade do Porto, Portugal

⁵ Faculdade de Ciências, Departamento de Biologia, Universidade do Porto, Portugal

⁶ ICBAS - Instituto de Ciências Biomédicas Abel Salazar, Universidade do Porto, Portugal

⁷ Plant Biochemistry, Faculty of Biology & Biotechnology, Ruhr University Bochum, D-44780 Bochum, Germany

⁸ University of Ljubljana, Faculty of Chemistry and Chemical Technology, University of Ljubljana, Večna pot 113, SI-1000 Ljubljana, Slovenia

⁹ ChELSI Institute, Department of Chemical and Biological Engineering, The University of Sheffield, Sheffield, UK

¹⁰ Plymouth Marine Laboratory, Prospect place, Plymouth, PL1 3DH, UK

¹¹ School of Chemical Engineering and Advanced Materials, c/- Faculty Office, Faculty of Science, Agriculture and Engineering, Newcastle University, Newcastle, NE1 7RU, UK

¹² Chaire de Bioinformatique, LGBA, Conservatoire National Des Arts Et Métiers, 75003 Paris, France

¹³ Instituto de Aplicaciones de las Tecnologías de la Información y de las Comunicaciones Avanzadas, Universitat Politècnica de València, Spain

¹⁴ Instituto Universitario de Matemática Pura y Aplicada, Universitat Politècnica de València, Spain

¹⁵ KSD Innovation GmbH, Werksstraße 15, 45527 Hattingen, Germany

¹⁶ Istituto per lo Studio degli Ecosistemi (ISE), Consiglio Nazionale delle Ricerche (CNR) via Madonna del Piano, 10, I-50019, Sesto Fiorentino, Italy

¹⁷ Escuela de Biología & Centro de Investigación en Ciencias del Mar y Limnología (CIMAR), Universidad de Costa Rica, San Pedro, San José 11501, Costa Rica

¹⁸ M₂M Engineering sas (M2M), Via Cinthia P.co S. Paolo, 13 Naples, Italy

61
62
63 **Abstract**
64

65 47 CyanoFactory, *Design, construction and demonstration of solar biofuel production using novel*
66 48 *(photo)synthetic cell factories*, was an R&D project developed in response to the FP7-
67 49 ENERGY- 2012-1 call “Future Emerging Technologies” and the need for significant advances
70 50 in both new science and technologies to convert solar energy into a fuel. CyanoFactory was an
71 51 example of “purpose driven” research and development with identified scientific goals which
72 52 also creates a new technology. The present overview highlights significant outcomes of the
73 53 project three years after its successful completion.
74
75

76 54
77
78 55 The scientific progress of CyanoFactory involved the: (i) Development of a ToolBox for
79 56 cyanobacterial synthetic biology, (ii) Construction of DataWarehouse/Bioinformatics web-
80 57 based capacities and functions, (iii) Improvement of chassis growth, functionality and
81 58 robustness, (iv) Introduction of custom designed genetic constructs into cyanobacteria, (v)
82 59 Improvement of photosynthetic efficiency towards hydrogen production, (vi) Biosafety
83 60 mechanisms, (vii) Analyses of the designed cyanobacterial cells to identify bottlenecks with
84 61 suggestions on further improvements, (viii) Metabolic modelling of engineered cells, (ix)
85 62 Development of an efficient laboratory scale photobioreactor unit, and (x) the Assembly and
86 63 experimental performance assessment of a larger (1350 L) outdoor flat panel photobioreactor
87 64 system during two seasons.
88
89
90
91
92
93

94 65
95 66 CyanoFactory - Custom design and purpose construction of microbial cells for the production
96 67 of desired products using synthetic biology – aimed to go beyond conventional paths to pursue
97 68 innovative and high impact goals. CyanoFactory brought together ten leading European
98 69 partners (universities, research organizations and enterprises) with a common goal – to develop
99 70 the future technologies *Synthetic biology* and *Advanced photobioreactors*.
100
101
102

103 71
104 72 A provisional patent application and subsequently a European Patent Request were submitted
105 73 covering construction and methods for the production of target molecules in a cyanobacterium.
106 74 From societal perspective, the article *Making-of Synthetic Biology: The European*
107 75 *CyanoFactory Research Consortium* (Wünschiers, 2016) was a contribution towards the
108 76 discussion about synthetic biology and its impact on our society.
109
110
111
112

113 77
114 78 Keywords: Cyanobacterial synthetic biology toolbox; DataWarehouse; Chassis robustness;
115 79 Biosafety; Improved electron chain; Large-scale photobioreactor cultivation
116
117
118

121
122
123 **80 1. Introduction**
124

125 81

126 82 CyanoFactory was a European research consortium with a global concept, whose aim was to
127
128 83 custom design, purpose construct and use the engineered cyanobacterial cells for the
129
130 84 production of a product. It involved highly cross-disciplinary complimentary competences
131
132 85 spanning many scientific disciplines and connected academia, engineering, entrepreneurship
133
134 86 and industry. This overview presents and discusses achievements in the European
135
136 87 CyanoFactory Consortium three years after its successful completion.
137

138 88

139 **89 2. ToolBox for cyanobacterial synthetic biology - Reliable transcription and translation**
140 **90 of heterologous genes in cyanobacteria**
141

142 91

143 92 The rapid advancement in molecular biology during the last decades, together with the drastic
144
145 93 drop in cost of DNA sequencing and synthesis, have allowed the development of advanced and
146
147 94 efficient tools for engineering and customization of microbial genomes. Most astonishing are
148
149 95 the advancements in genetic engineering of the most common model organisms, like
150
151 96 *Escherichia coli* (*E. coli*), where libraries of well characterized genetic devices and parts enable
152
153 97 quick and reliable construction of recombinant strains with desired properties. In cyanobacteria,
154
155 98 the knowledge and availability of genetic tools and standardized biological parts are far behind
156
157 99 in comparison to the traditional model organisms. In recent years, advancements in this
100
101 100 research field have started to enhance our ability to modify and engineer cyanobacterial
102
103 101 genomes in a predictable and reliable way.

104 102

105 103 A key feature for successful modification or redesign of any cellular machinery or function in
106
107 104 any biological system is the tuning of expression level of a given gene. Much attention was
108
109 105 therefore given to the characterization and development of promoter regions, and an increasing
110
111 106 number of promoters of different strengths, both constitutive and inducible, are available for
112
113 107 the more commonly used cyanobacterial strains. Up to this date, the larger part of heterologous
114
115 108 expressions attempts in cyanobacteria have used endogenous promoters. A number of
116
117 109 interesting chemicals have been successfully produced in cyanobacteria, using overexpression
118
119 110 from these natively occurring promoters (Zhou et al., 2014). Due to their driving of high
120
121 111 transcription levels, promoter regions related to light harvesting complex and photosystems,
122
123 112 such as *Pcpc* and *PsbA*, have been widely used. Improved variants of the *Pcpc* in *Synechocystis*
124
125 113 PCC 6803 (henceforth *Synechocystis* 6803) have been shown to enable very high yields of
126
127

181
182
183
184
185
186
187
188
189
190
191
192
193
194
195
196
197
198
199
200
201
202
203
204
205
206
207
208
209
210
211
212
213
214
215
216
217
218
219
220
221
222
223
224
225
226
227
228
229
230
231
232
233
234
235
236
237
238
239
240

114 heterologously expressed proteins (Ramey, Barón-Sola, Aucoin, & Boyle, 2015; Zhou, Zhu,
115 Cai, & Li, 2016). Although often resulting in high levels of expression, the light regulated
116 nature of these promoters can make them unsuitable for usage under differing and low light
117 conditions.

118
119 To address the lack of well characterized promoters with more modest expression levels, a
120 library of constitutive promoters based on *Pcpc* from *Synechocystis* 6803 was developed for
121 the closely related *Synechococcus* PCC 7002 (Markley et. al., 2015). By truncation and
122 randomized mutagenesis, a wide variety of promoters with different strengths were developed
123 and shown to span three orders of magnitude in expression levels using a yellow florescent
124 protein (YFP) reporter. Moreover, the developed promoters are reported to be decoupled from
125 the light regulation that hampers the original promoter sequence.

126
127 Other endogenous promoters used for synthetic biology approaches in cyanobacteria include a
128 number of micronutrient and metal induced promoters. These promoters are favorable in many
129 applications due to their inducible nature and wide dynamic range. Apart from endogenous
130 promoters, modified inducible promoter systems from *E. coli* have been successfully
131 introduced and employed in cyanobacteria. Although well studied inducible promoters, such
132 as *Plac* and *Ptet* from *E. coli* have proven to function poorly in cyanobacteria (Huang, Camsund,
133 Lindblad, & Heidorn, 2010), later efforts to adapt non-native induction systems to
134 cyanobacterial hosts have yielded promising results. A TetR-regulated promoter system has
135 been developed for cyanobacteria, displaying a wide induction range (Ramey et al., 2015).
136 Efforts have been also made to introduce isopropyl β -D-1-thiogalactopyranoside (IPTG)-
137 inducible transcription initiation systems. Two lac operated promoters, *PtrcO1* and *PtrcO2*,
138 were introduced and tested in *Synechocystis* 6803 (Huang et al., 2010). Both exhibited high
139 activity in the cyanobacterial host, although *Ptrc* was not well repressed by LacI and *PtrcO2*
140 could not be effectively induced by IPTG. By using a combination of the endogenous *Pcpc*
141 from *Synechocystis* 6803 and *E. coli* promoter libraries, Markley et al. developed a library of
142 IPTG inducible promoters in *Synechococcus* PCC 7002, where the top performer exhibited a
143 48-fold increase in expression level of the reporter gene upon induction (Markley et al., 2015).
144 In addition, a set of synthetic promoters whose design was based on the well characterized
145 *PpsbA2*, *Ptrc*, *Ptacl* and *PT7* (some including operator sequences for regulatory proteins) were
146 developed. For the characterization of the promoters in *Synechocystis* PCC 6803, the devices
147 were assembled to include a *gfp* reporter, and the *Synechocystis* 6803 *PrnpB* was used as a

241
242
243 148 reference (Huang et al 2010). The results showed a range of functional synthetic promoters
244
245 149 with strengths varying from 0.13- to 41-fold compared to *PrnpB* (Ferreira et al., 2018). Figure
246
247 150 1 shows confocal micrographs of *Synechocystis* mutants exhibiting differential *gfp* expression
248
249 151 depending on the promoter used. These regulatory elements can be used for the construction
250
251 152 of synthetic devices/circuits for introduction into the photoautotrophic chassis.

252
253 154 A predictable and tunable initiation of transcription is not the only component of well-
254
255 155 controlled gene expression. The initiation of translation via the attachment of the ribosome to
256
257 156 the ribosome binding site (RBS) of the mRNA is also key in expression regulation. Most
258
259 157 examples of heterologous gene expression in cyanobacteria have reported the usage of native
260
261 158 RBS sequences, commonly the one associated with the promoter used for expression. In 2011,
262
263 159 Heidorn et al. developed RBS* for synthetic biology approaches in cyanobacteria, which
264
265 160 widely outperformed three commonly used RBSs in terms of expression level of a reporter
266
267 161 gene in *Synechocystis* 6803 (Heidorn et al., 2011). Also, an 11-member RBS library with a 30-
268
269 162 fold range in expression levels has been developed for and analyzed in *Synechococcus* PCC
270
271 163 7002 (Markley et al., 2015).

272
273 164
274 165 The fact that quantitative expression levels from a given transcription and translation initiation
275
276 166 unit can differ greatly depending on the genetic context has presented an obstacle for further
277
278 167 advancement towards tunable and predictable gene expression (Cardinale & Arkin, 2012). This
279
280 168 phenomenon is speculated to result from different mRNAs forming different secondary
281
282 169 structures in and around the 5'-untranslated region (5'-UTR), hiding the RBS in varying and
283
284 170 unpredictable ways (Mutalik et al., 2013). It has been shown in *E. coli* that this unpredictability
285
286 171 can be largely overcome by the usage of insulator sequences, like the bicistronic design (BCD)
287
288 172 described by Mutalik et al., where the RBS of the gene of interest (GOI) is included in a short
289
290 173 upstream ORF (Mutalik et al., 2013). This design permits temporary melting of RNA
291
292 174 secondary structures in the junction between the 5'UTR and the GOI by the translation of the
293
294 175 leader peptide, ensuring availability of the RBS for translation initiation and providing a more
295
296 176 reliable gene expression (Mutalik et al., 2013). We used BCD-insulation to enable expression
297
298 177 of two synthetic constructs in *Synechocystis* 6803, which yielded very low protein levels when
299
300 178 expressed with a traditional monocistronic design assembled from standardized biological
179 parts.

301
302
303 181 The *PtrcOI*-RBS* and *PtrcOI*-B0034 (BBa_B0034, Registry of Standard Biological Parts)
304
305 182 expression units have been shown to function well in unicellular cyanobacterium *Synechocystis*
306 183 6803 when employed upstream of a reporter gene (Heidorn et al., 2011). However, when using
307
308 184 these rational synthetic biology designs to express other heterologous genes in *Synechocystis*
309
310 185 6803, we observed considerable variation in expression levels from the same transcription and
311
312 186 translation initiation unit in the presence of different GOIs. We cloned *PtrcOI*-RBS* upstream
313
314 187 the codon-optimized *hydA* from *Chlamydomonas reinhardtii* and *PtrcOI*- B0034 upstream of
315
316 188 the codon-optimized, flag-tagged, *hydEFG* operon from *Clostridium acetobutalicum*, and
317
318 189 transformed these constructs into both *E. coli* strain DH5 α (henceforth *E. coli*) and
319
320 190 *Synechocystis* 6803, using the self-replicating broad host shuttle vector pPMQAK1 (Huang et
321
322 191 al., 2010). Corresponding constructs with translation initiation elements replaced with the
323
324 192 BCD2-sequence (only the first element when constructing the operon) (Mutalik et al., 2013)
325
326 193 were also developed and transformed in a similar fashion. SDS-PAGE and Western
327
328 194 immunoblot analyses of extracted proteins from *Synechocystis* 6803 revealed expression from
329
330 195 the *hydA*-gene only in the BCD construct (Figure 2A). Expression of the flag tagged HydG
331
332 196 protein from the *hydEFG* operon was barely detectable from the monocistronic construct, but
333
334 197 strongly evident from the BCD counterpart (Figure 2B). Similar Western blot analyses of the
335
336 198 *E. coli* strains revealed protein expression from all constructs, monocistronic and bicistronic
337
338 199 alike (Figures 2C and 2D), but with notably higher expression levels from BCD-*hydA* than
339
340 200 from the corresponding monocistronic construct. Transcription analysis by reverse-
341
342 201 transcriptase polymerase chain reaction (RT-PCR) and gel electrophoresis confirmed transcript
343
344 202 presence in all *Synechocystis* 6803 constructs (Figure 3) and revealed no visible differences in
345
346 203 transcript levels between the monocistronic and bicistronic designs.
347
348 204

349
350 205 Our results highlight the unpredictability of using biological parts in different genetic contexts,
351
352 206 especially in cyanobacteria. Even though the monocistronic expression designs used in our
353
354 207 investigation had proven to be functional for heterologous expression in *Synechocystis* 6803
355
356 208 (Huang et al., 2010), the change of GOI totally changed the performance of the promoter/RBS
357
358 209 combinations, resulting in our case in protein levels below satisfactory for biological
359
360 210 applications. The presence of transcripts from the monocistronic expression constructs in
211
212 *Synechocystis* 6803 (Figure 2), together with the very low or undetectable levels of protein
213
214 (Figures 2A and 2B) led us to conclude that inefficient translation may be causing the
remarkably low expression levels compared to corresponding levels in *E. coli*. It is evident
from our results that employment of a BCD-adapter in cyanobacteria can aid to express

361
362
363 215 heterologous proteins in satisfactory amounts, in a genetic context where a traditional synthetic
364
365 216 biology design fails to do so. In the case of the *hydEFG* operon in *Synechocystis* PCC 6803,
366
367 217 the insertion of a BCD-adaptor between the promoter and the first gene of the operon (*hydE*)
368
369 218 enabled translation of the last gene (*hydG*) (Figure 3B). This result suggests that one BCD-
370
371 219 adaptor following the promoter is enough to enable efficient translation of the whole operon.
372
373 220 Indeed, the presence of both HydE and HydF was later confirmed by proteomic analysis (data
374
375 221 not shown). We speculate that the distance between the stop codons of *hydE* and *hydG* and the
376
377 222 RBSs of the following genes (11 bp in our construct) is short enough for the ribosome to disrupt
378
379 223 possible secondary RNA structures in the following RBS:GOI junctions.

379 224
380 225 Using the developed synthetic biology tools, a synthetic *in vivo* activation of a heterologously
381
382 226 expressed [FeFe]-hydrogenase in the unicellular cyanobacterium *Synechocystis* PCC 6803 was
383
384 227 recently demonstrated (Wegelius et al 2018). The non-native, semi-synthetic enzyme not only
385
386 228 functioned in the cells but also linked to the native metabolism where the activated hydrogenase
387
388 229 evolved hydrogen both in light and in darkness.

387 230

388 231 **3. Improvement of chassis growth, functionality and robustness**

389 232

390 233 Aiming at the stable integration of synthetic devices into the *Synechocystis* 6803 chromosome,
391
392 234 several genomic neutral sites were identified. Disruption mutants in those *loci* were generated
393
394 235 and extensively characterized in terms of fitness, transcription and proteomics, validating the
395
396 236 neutrality and functionality of these sites. The constructed integrative vectors include
397
398 237 BioBrick-compatible multiple cloning sites flanked by transcription terminators, constituting
399
400 238 robust and insulated cloning interfaces. The mutants and vectors generated are available and
401
402 239 can be used for synthetic biology approaches (Figure 4; (Pinto et al., 2015), Portuguese
403
404 240 Provisional Patent #108564/European Patent Request #16175360.3, P274.4 EP).

405 241

406 242 With the aim of improving chassis robustness, a set of targets (candidate genes/pathways) was
407
408 243 identified leading to the improvement strategies focusing on heat shock response proteins
409
410 244 (HSP) and compatible solutes (CS) synthesis. Several devices were constructed using synthetic
411
412 245 promoters developed within CyanoFactory and implemented in *Synechocystis* 6803. Some of
413
414 246 the generated mutants exhibited a remarkable increase in the transcription of genes encoding
415
416 247 compatible solutes, e.g. the enzymes responsible for glucosylglycerol production - *ggpS* and
417
418 248 *ggpP* - even without NaCl supplementation. The increase in compatible solute production is

421
422
423 249 being evaluated by NMR. In addition, iTRAQ and RNA-seq studies were performed and data
424
425 250 analysis is being performed (IBMC-Instituto de Biologia Molecular e Celular in collaboration
426
427 251 with University of Sheffield).

428 252
429
430 253 Furthermore, the chassis functionality and robustness were also assessed by inactivating
431 254 *slr1270* which encodes a TolC homologue. TolC is an outer membrane protein associated to
432
433 255 biomolecule secretion, including proteins and endo- and/or exogenous metabolites. Our results
434
435 256 show that the TolC-like Slr1270 bestows a marked physiological fitness to *Synechocystis* 6803.
436 257 Moreover, our work presents a valuable model for studying outer membrane vesicle (OMV)
437
438 258 formation and release (Oliveira et al., 2016). In the future, OMVs and optimized secretion
439 259 system(s) can be used as tools to increase the functionality of a chassis based on *Synechocystis*
440
441 260 6803.

442 261
443
444 262 For modulation of the chassis intracellular oxygen concentration, important when introducing
445
446 263 synthetic modules encoding O₂-sensitive enzymes (such as hydrogenases), several Oxygen
447 264 Consuming Devices (OCD) were designed and synthesized. The OCDs are comprised of the
448
449 265 *cueO* encoding *E. coli*'s native laccase and its variants (with improved activity), preceded by
450 266 the F2620 BioBrick, which allows inducible expression of the device by adding acyl-
451
452 267 homoserine lactone. These devices were characterized *in vitro* in *E. coli* (protein crude extracts).
453
454 268 Assessment of the specific laccase activity and oxygen consumption rate revealed that the
455 269 OCDs are functional in all conditions tested. Moreover, characterization of the OCDs *in vivo*
456
457 270 using *E. coli* cells confirmed the consumption of O₂ in cells that harbored the devices (Pacheco
458
459 271 et al., 2018) (Figure 5).

460 272 461 273 **4. Improving electron flow towards H₂ production**

462 274
463
464 275 For efficient production of hydrogen, cyanobacterial metabolism of electron acquisition and
465
466 276 distribution has to be engineered. Key players of the optimization process are Photosystem II
467
468 277 (PSII), Ferredoxin-NADP-Oxido-Reductase (FNR), and ATP synthase (Figure 6).

469 278
470
471 279 For an increase in the supply of reduction equivalents, the starting-point for the optimization
472
473 280 is the water splitting process. Importantly, we have shown that the introduction of electrons
474
475 281 into the photosynthetic electron transport chain is significantly increased in phycobilisome
476 282 mutants with reduced light harvesting antennas (Kwon, Bernát, Wagner, Rögner, & Rexroth,
477
478

481
482
483 283 2013). Besides increasing the amount of PSII per cell, higher cell densities in photobioreactors
484
485 284 are also obtained, which further increase the space-time yield of the process. While the positive
486
487 285 impact of a truncated phycobilisome structure on linear electron transport was observed in the
488
489 286 Olive mutant, reports on lower performance of phycocyanin deletion mutants were published
490
491 287 by other investigations (Page, Liberton, & Pakrasi, 2012).
492

493 288
494 289 As the Olive mutant with a truncated phycobilisome as its main characteristic had been
495 290 generated by chemically induced random mutagenesis in 1989 and had an unclear genomic
496 291 background, the complete genome of the Olive mutant was analyzed by next-generation
497 292 sequencing. The results of the sequencing activity display a frame-shift within the *cpcB* gene.
498 293 While this leads to a loss of function on the protein level and explains the truncation of the
499 294 light-harvesting antenna, on RNA and DNA levels the gene remains virtually unchanged. This
500 295 might suggest a role of regulatory RNAs, which are thought to play an important role in the
501 296 transcriptional regulation of the light-harvesting apparatus, to explain the differences in the
502 297 phenotype of the rational phycobilisome truncation mutants and the Olive mutant.
503
504
505
506

507 298
508 299 In addition to truncation of the light-harvesting antenna, partial decoupling of the ATP synthase
509 300 was identified as a route for increasing photosynthetic electron transport. For a further increase
510 301 in electron transport rate, the deletion of the C-terminal domain of ATP synthase subunit ϵ ,
511 302 which was shown to accelerate photosynthetic electron transport (Imashimizu et al., 2011), was
512 303 introduced into the Olive mutant. The resulting Olive- $\Delta C\epsilon$ mutant displayed a fourfold
513 304 increased electron transport rate in comparison with the wild type. However, only 25% of the
514 305 electrons produced in the Olive- $\Delta C\epsilon$ mutant are transferred into the cyanobacterial
515 306 metabolism, while 75 % are transferred to O_2 in the Mehler reaction catalyzed by the
516 307 flavodiiron protein Flv1 and Flv3. If these electrons can be redirected to a hydrogenase, a future
517 308 H_2 -production would not be in competition with the demands of the metabolism.
518
519
520
521
522
523
524

525 309
526
527
528
529
530
531
532
533
534
535
536
537
538
539
540

541
542
543 310 Re-routing of the reduction equivalents is a key step for the integration of the hydrogenase into
544
545 311 the cyanobacterial metabolism, the flux of reduction equivalents has to be redesigned. In the
546
547 312 focus of this design process is the Ferredoxin-NADP-Oxido-Reductase (FNR), as it transfers
548
549 313 the main share of reduction equivalent towards carbon fixation. Based on the structural
550
551 314 information (Liauw et al., 2012), rational design variants of the FNR with reduced ferredoxin
552
553 315 affinity were created and screened for their activity by two independent *in vitro* assays (Figure
554
555 316 7, Table 1) – a cytochrome c reduction assay and light-activated proflavin assay with a direct
556
557 317 competition of hydrogenase and FNR for reduced ferredoxin.

558
559 318
560 319 Based on the cytochrome c reduction assay, FNR variants K78D, K75A-K78D and K75D-
561
562 320 K78D show a very low cytochrome reduction rate compared to the wild-type protein. This low
563
564 321 electron transfer efficiency is also confirmed by the competition experiment. Forty to sixty
565
566 322 percent of the electrons are transferred to hydrogenase when FNR variants K78D, K75A-K78D
567
568 323 and K75D-K78D compete with the [FeFe] hydrogenase from *Chlamydomonas reinhardtii*,
569
570 324 while only 5% are used for hydrogen production when the wild-type FNR is used for the
571
572 325 experiment. An additional improvement was achieved by the allocation of specific interaction
573
574 326 residues by NMR analysis. This approach led to a combined construction of Fd- and FNR-
575
576 327 mutants which enabled an about 18-fold enhanced electron flow from Fd to HydA1 in *in vitro*
577
578 328 assays (Wiegand et al. 2018). The negative impact of these mutations on the Fd-FNR electron
579
580 329 transport was dominated by the FNR variants (up to 42 %), but also Fd-variants contributed up
581
582 330 to 23 %, and surprisingly had in parallel a direct positive impact on the Fd-HydA1 electron
583
584 331 transport (up to 23 %). This is an excellent basis for the construction of a hydrogen-producing
585
586 332 design cell and the study of photosynthetic efficiency-optimization with cyanobacteria.

587 333

588 334 **5. A synthetic biology approach to biosafety of genetically modified cyanobacteria**

589 335

590
591 336 Currently, cyanobacterial biotechnology is building on wild-type strains that were at one time
592
593 337 isolated from nature. Genetic modifications towards improving the performance of these strains
594
595 338 are focused on introduction of new biosynthetic pathways, while biosafety issues tend to be
596
597 339 put aside. However, especially in synthetic biology, there has been a pronounced concern from
598
599 340 the public as well as scientists about biosafety, therefore we decided to implement a biosafety
600
341 device into *Synechocystis* 6803 that would present a biological barrier against the spread of
342 genetically modified *Synechocystis* cells into the environment.
343

601
602
603 344 In principle, there are many different approaches for improving biosafety of genetically
604 345 modified microorganisms, as reviewed specifically for synthetic biology elsewhere (Wright,
606 346 Stan, & Ellis, 2013). For our needs, an active containment strategy seemed the best option. It
608 347 relies on an introduced kill-switch device that enables controlled killing of only those
609 348 engineered microorganisms that carry the device. This type of devices had been implemented
611 349 previously in some bacterial species, but only recently have we implemented them in
613 350 cyanobacteria (Čelešnik et al., 2016).

614 351
616 352 For the cyanobacterial kill-switch we envisaged that it should be based as much as possible on
617 353 cyanobacterial own genetic elements (to minimize transgene use), should be induced
619 354 specifically by using low molecular weight compounds that are easily available, could be used
621 355 in large-scale experiments, and should trigger cell death from within the cell, leaving other
622 356 organisms in the environment unaffected as much as possible.

624 357
626 358 Two approaches were examined, one based on a toxin/antitoxin system (TAS) and the other on
627 359 a nuclease/nuclease inhibitor system (NIS). Both are intrinsic cyanobacterial regulatory
628 360 systems with specific physiological roles in coping with stress (TAS) and serving for
629 361 nutritional purposes or sometimes as bacteriocides (NIS). In the first approach, we constructed
632 362 two recombinant strains by rewiring two related TAS pairs originating from *Synechocystis*
633 363 6803 reviewed in Kopfmann et. al., (Kopfmann, Roesch, & Hess, 2016) and reintroducing the
635 364 resulting two circuits into the originating strains. Toxin/antitoxin pairs Ssr1114/Slr0664 and
636 365 Slr6101/Slr6100 are originally encoded as single operons in which protein products act as
638 366 transcription regulators. For the construction of biosafety devices (Figure 8), the toxin- and
639 367 antitoxin-encoding units were placed under separate promoters, which were either constitutive
641 368 or inducible. In the second approach, we took advantage of the non-specific nuclease NucA
643 369 and its cognate inhibitor NuiA originating from the filamentous cyanobacterium *Anabaena* sp.
645 370 PCC 7120 (Muro-Pastor, Flores, Herrero, & Wolk, 1992). Selected options for reorganization
646 371 of wild-type operons are presented in Figure 8.

648 372
649 373 In our work, we limited the choice of promoters to those that respond to metal ions, bearing in
651 374 mind that the cost of inducer compounds should be kept low in large-scale biotechnological
652 375 applications. Since heavy metals are actually quite toxic to cyanobacteria, we searched for
654 376 metal inducers that are active in subtoxic concentrations, allowing for selective killing of only
655 377 those cyanobacteria that carry synthetic biology suicide switches. All the kill-switches tested

661
662
663 378 contained a constitutive and an inducible promoter, regardless of the type of effector/inhibitor
664
665 379 pair and the approach (Figures 8B-D). Of the known inducible promoters, we tested the copper-
666
667 380 or zinc-inducible *copB* and *copM* promoters, the zinc-inducible *smtA* promoter and the nickel-
668
669 381 inducible *nrsB* promoter, all from *Synechocystis* 6803. Constitutive promoters that we tested
670
671 382 were *rnpB* (RNaseP subunit B), and *rbcL1A* (RuBisCO large subunit), promoters from the
672
673 383 same strain. Due to high copper toxicity, best results were obtained by zinc induction.

674
675 385 Since there is limited data available on promoter behaviour in *Synechocystis* 6803, several
676
677 386 optimized constructs had to be developed to achieve the necessary fine-tuning of devices that
678
679 387 resulted in efficient induced cell killing. Promoter combinations were investigated with both a
680
681 388 nuclease/nuclease inhibitor system (NIS) and a toxin/antitoxin system (TAS) in different
682
683 389 combinations with device construction and, see Table 2.

684
685 391 With the *copM* and *nrsB* promoters, full-length and shortened promoter versions were tested.
686
687 392 Additional contribution towards improved device behaviour was achieved by replacing the
688
689 393 native RBS with a synthetic one, as well as by introduction of a BCD arrangement (Mutalik et
690
691 394 al., 2013), the aforementioned specific insulator sequence that facilitates reliable translation
692
693 395 initiation of random downstream genes. Additionally, fusion of degradation tags to the C-
694
695 396 terminus of the toxic effectors helped curtail and thereby optimize effector cellular
696
697 397 concentration - in many cases this was the only way to clone the toxin genes at all due to the
698
699 398 high toxicity for the heterologous *E. coli* host.

700
701 400 Although in perspective the suicide device would likely be best positioned on the chromosome,
702
703 401 we completed all the experiments with the previously developed broad-host expression plasmid
704
705 402 pPMQAK (Huang et al., 2010). This enabled us to test the constructs faster, since segregation
706
707 403 of clones after genomic incorporation of the constructs could be avoided.

708
709 404
710
711 405 The effectiveness of the genetic constructs in *Synechocystis* 6803 was monitored by RT-PCR
712
713 406 to assess effector expression in the presence of inducer (and expression leakiness in inducer
714
715 407 absence), and by screening the growth rates and viability of recombinant cyanobacterial strains.
716
717 408 We found out that TAS-based devices had either no effect on cell growth or caused only a
718
719 409 bacteriostatic effect. Since a bactericidal effect would be preferred, we sought other
720
721 410 combinations of genetic elements. Only one of these proved to be potentially useful for
722
723 411 application in synthetic biology and biotechnology. It consisted of a bicistronic arrangement

721
722
723 412 downstream of the prolonged *copM* promoter, which was linked to the NucA nuclease coding
724
725 413 region. From the coding region, the nuclease signal peptide had been removed, while a C-
726
727 414 terminal T1 degradation tag had been added. The NuiA inhibitor coding region was joined to
728
729 415 the *rnpB* promoter fused to a synthetic ribosome binding site (Figure 7D). The presence of the
730
731 416 inhibitor in the kill-switch helped ensure that any unwanted leakage of the toxic effector was
732
733 417 neutralized in the cell.

734
735 418
736 419 Cyanobacteria with the best-performing device repeatedly displayed cell killing in culture
737
738 420 when induced by 12-14 μM Zn^{2+} ions, which was visible by naked eye and later confirmed by
739
740 421 cell viability assay (the MTT test), growth curve analysis and RT-PCR. We believe that this
741
742 422 construct could be further optimized for robustness and tested at higher cell densities and under
743
744 423 simulated outdoor conditions. Finally, we would like to note that the nuclease-based suicide
745
746 424 device that we developed and tested is not only a cell-killing synthetic biology circuit, but also
747
748 425 a potential shredder of (recombinant) DNA. This way, the risk of spread of transgenes into the
749
750 426 environment is further reduced.

751 427 752 428 **6. Analyses of the purpose designed cyanobacterial cells to identify bottlenecks and** 753 429 **suggest further improvements**

754 430
755 431 During CyanoFactory, a number of the challenges affecting the development of *Synechocystis*
756
757 432 as a synthetic biology and biotechnology production platform were assessed; primarily with
758
759 433 proteomics, but also with transcriptomics and ^{13}C metabolic flux analysis. The aim of this
760
761 434 systems-level approach was two-fold; first it provided insight into the system of responses the
762
763 435 cell produces to the genetic and environmental factors studied in the project; and second it
764
765 436 enabled monitoring of the flow of metabolites through the cell to give an impression of reaction
766
767 437 rates. Both of these outputs enabled rational design choices to be made based on the
768
769 438 intracellular response of the cell, when combined with an in-silico model of the organism. In
770
771 439 addition to the use of these techniques for assessing the system, a number of key developments
772
773 440 for the methods were also conducted over the course of the project, to improve the quality of
774
775 441 the data and to facilitate its upgrade into knowledge.

776
777 442
778 443 Proteomics is the study of the protein complement within a system, where a population of cells
779
780 444 are (usually) measured quantitatively at a single point in time to give a snap-shot impression

781
782
783 445 of the protein-level cellular response (Altelaar et al., 2013). Whilst the whole proteome and its
784
785 446 various interactions and post-translational modifications are poorly understood, comparing an
786
787 447 engineered system to a control condition enables us to identify unexpected or off-target
788
789 448 responses to a design (and potential 'bottlenecks'). This technique is incredibly powerful, and
790
791 449 is gaining popularity for assessment of industrially relevant organisms and processes. Groups
792
793 450 working to develop multi-omics are starting to bridge the gap between the most powerful
794
795 451 proteomic techniques and production strain analysis in, for example, *E. coli* (Brunk et al., 2016).

796 452
796 453 Prior to method development, the existing literature relating to *Synechocystis* 6803 (for
797
798 454 consistent naming throughout the paper) and the leading-edge developments in proteomics for
799
800 455 production strains were analyzed for trends and gaps (Landels, Evans, Noirel, & Wright, 2015).
801
802 456 A number of improvements to the physical and analytical methodology were identified,
803
804 457 including the extraction method used for collecting proteins, the quality assessment techniques,
805
806 458 and the grouping (e.g. gene ontology, metabolic mapping and clustering of cellular functions)
807
808 459 and analysis of the large datasets. *Synechocystis* 6803 is strongly placed as a flagship organism
809
810 460 for systems-level design of photosynthetic synthetic biology, as it was the third living system
811
812 461 to have its genome sequenced and the first photosynthetic organism to be sequenced.

813 462
813 463 The latest studies using the most advanced techniques and machinery enable just over 60% of
814
815 464 the predicted proteins in the proteome to be identified and quantified rapidly and with
816
817 465 confidence. Due to the complex membrane structure, one of the major hurdles to a more
818
819 466 complete analysis is reproducible cell lysis and protein collection. A literature analysis, with
820
821 467 experimental verification, demonstrated that a combination of sonication and bead-beating
822
823 468 steps for protein extraction provided the most effective extraction technique. It provided more
824
825 469 reliable results than liquid nitrogen cracking in a mortar with pestle, which gave variable output
826
827 470 and was highly operator dependent, and avoided issues found with pressure-related and freeze-
828
829 471 thaw methodologies – both of which *Synechocystis* 6803 was found to be resistant to. Notably,
830
831 472 for a less hardy organism these techniques could lead to protein damage and reduced data
832
833 473 quality.

834 474
834 475 As a photosynthetic microorganism, one of the major constituents of the *Synechocystis* 6803
835
836 476 cell is a thylakoid membrane system loaded with photosynthetic machinery referred to here as
837
838 477 'antenna proteins'. For context, close to 60% of the organism is protein by mass, and over 20%
839
840 478 of this mass is solely the photosynthetic machinery. These high abundance antennae proteins

841
842
843 479 found in *Synechocystis* cause issues for analysis as they form the majority of the sample,
844
845 480 effectively reducing what is referred to as the ‘dynamic range’ or the difference in
846
847 481 concentration between the most abundant and least abundant proteins – the result is repeated
848
849 482 identification and quantification of these proteins by the mass spectrometer to the exclusion of
850
851 483 many lower abundance proteins. This can be mitigated to a certain extent by using liquid
852
853 484 chromatography to separate and concentrate peptides during analysis, giving better quality data.
854
855 485 It was found that using a hypercarb HPLC separation yielded a more effective separation of
856
857 486 peptides than either strong cation exchange (SCX) or HILIC. In addition, it was found that the
858
859 487 wavelengths of light absorbed by the light-responsive or light-harvesting proteins caused
860
861 488 problems with typical spectrophotometric analyses used for protein quantification, such as a
862
863 489 Bradford assay – repeat analyses on the same sample had widely varying results. Alternative
864
865 490 techniques are required to minimize this issue (Kalb & Bernlohr, 1977).
866
867 491

868
869 492 To further improve the organism for future synthetic biology developments a range of different
870
871 493 investigations were carried out. Firstly, an analysis was performed on a series of neutral
872
873 494 integration sites within the *Synechocystis* genome. A number of key sites were found to
874
875 495 generate no unexpected background protein expression within *Synechocystis* and as a result are
876
877 496 suitable for stable integration of synthetic constructs (Pinto et al., 2015). These sites were tested
878
879 497 with an antibacterial resistance cassette, which was shown to affect expression of only a single
880
881 498 protein of unknown function. Secondly, to better understand the flow of carbon through the
882
883 499 cell when comparing an antenna mutant (Olive) with the wild type cells, a transient ¹³C
884
885 500 labelling experiment was performed with a corresponding quantitative proteomic analysis. A
886
887 501 third major experimental program was undertaken to assess the organism in a pilot-scale
888
889 502 environment. A quantitative proteomic assessment of *Synechocystis* found that whilst the
890
891 503 background proteomic state appeared to vary significantly between repeated runs in our 1350
892
893 504 L scale PBR system, systematic changes were observed through the passage of the day.
894
895 505

896 506 **7. Metabolic modelling of the engineered cells**

897
898
899 507
900 508 Rational design of living organisms for biotechnological purposes is a challenging
901
902 509 interdisciplinary effort which can be supported by *in silico* analysis. Modelling strategies serve
903
904 510 as a basis for unravelling the underlying mechanisms responsible for cell behavior and allow
905
906 511 theoretical assessment of environmental and genetic variations, whereas laboratory
907
908 512 experiments are often expensive, time demanding or shed light on just a specific process of the

901
902
903 513 system. Engineering cyanobacteria for producing metabolites of interest, such as hydrogen,
904 514 entails an overall knowledge of metabolism but also a detailed comprehension of
905 515 photosynthesis in particular. Additionally, the application at industrial-scale requires a specific
906 516 search for optimal growth conditions in designed photobioreactor frameworks.
907
908
909
910 517

911 518 In order to understand the biochemical processes occurring within a *Synechocystis* cell,
912 519 metabolic models of the strains of interest are needed. The departing point to build an accurate,
913 520 up-to-date, genome-scale metabolic model of *Synechocystis* 6803 was a model previously
914 521 developed, iSyn811 (Montagud et al., 2011; Montagud, Navarro, Fernández de Córdoba,
915 522 Urchueguía, & Patil, 2010). More than 200 reactions were added and/or updated leading to
916 523 significant improvements in simulations, such as greater plasticity, better accuracy at
917 524 representing electron consuming pathways and a more realistic quantification of cell's energy
918 525 needs, which yield more precise metabolic characterization of the strains and enhance the
919 526 predictability of the model. The improved model can be considered as our “reference” for wild
920 527 type *Synechocystis* 6803. However, other wild type or mutant strains have also shown
921 528 interesting properties, therefore derivative models are required to study them. We have
922 529 developed a pipeline that aims at the elucidation of how differences in sequence might affect
923 530 the metabolic function of these strains, allowing the construction of models for the new strains
924 531 based on the original one.
925
926
927
928
929
930
931
932
933
934 532

935 533 These metabolic models can serve to guide strain design by assessing how different
936 534 modifications in media or genomes can improve growth or productivity of desired metabolites.
937 535 In that sense, a substrate study was performed to determine the best sources of inorganic
938 536 nitrogen and sulfur in terms of hydrogen production. In the case of nitrogen, the results obtained
939 537 from the simulations qualitatively matched previous experimental observations (Baebprasert,
940 538 Jantaro, Khetkorn, Lindblad, & Incharoensakdi, 2011; Gutthann, Egert, Marques, & Appel,
941 539 2007), while regarding sulfur, this is, to our knowledge, the first work in which different
942 540 sources have been tested to improve hydrogen production. Altogether, the results of this study
943 541 showed that by choosing the appropriate source among these inorganic substrates, maximum
944 542 optimal H₂ production can be substantially increased (Figure 9). As a further application,
945 543 genetic changes were analyzed in order to choose the best option between some candidates for
946 544 the synthesis of compatible solutes. The results of this study showed that in terms of metabolic
947 545 cost, glycine betaine is the less resource-consuming and therefore the best possible between
948 546 the proposed options, as greater production of the solute is possible at equal growth rates. Both
949
950
951
952
953
954
955
956
957
958
959
960

961
962
963 547 case studies exemplify how, by means of metabolic simulations, support can be given to
964
965 548 experimentalists in the selection of the best environmental and genetic conditions enabling
966
967 549 enhanced H₂ production.
968

969 550
970 551 Although classic metabolic simulations appropriately solve some biotechnological problems,
971
972 552 nowadays with the advent of high-throughput technologies, the field of systems biology has
973
974 553 amassed plentiful omics data that can be combined with metabolic models to heighten the
975
976 554 predictive capabilities of computational simulations and their plasticity when dealing with
977
978 555 perturbed conditions. After carefully considering different options in terms of available
979
980 556 information and computational cost, we finally decided to implement a previously described
981
982 557 methodology, IOMA (Yizhak, Benyamini, Liebermeister, Ruppin, & Shlomi, 2010), in which
983
984 558 proteomics, metabolomics and kinetic parameters, are integrated into metabolic simulations.
985
986 559 This scheme allows to qualitatively improve the simulations' response to environmental
987
988 560 changes, depending on the quality and amount of available experimental information. A further
989
990 561 development, META-MODE, is an algorithm that performs multi-objective optimizations of a
991
992 562 genome-scale metabolic model allowing the use of biologically-relevant non-linear constraints
993
994 563 and that, with the inclusion of experimental flux data, permits researchers to have realistic
995
996 564 metabolic simulations without having to impose constraints that are tiresome to find and even
997
998 565 sometimes cryptic to understand. With META-MODE, simulations can be driven maximizing
999
1000 566 growth without stating any biomass equation, so that different biomass compositions will be
1001
1002 567 obtained depending on the conditions. Our final goal is to incorporate different algorithms into
1003
1004 568 META-MODE, leading to a comprehensive tool prepared for different omics integration that
1005
1006 569 performs advanced metabolic simulations.
1007

1008 570
1009 571 A further goal within CyanoFactory was the construction of a kinetic model of photosynthesis,
1010
1011 572 as this process is highly dynamic, regulated and drives the main energetic pools in autotrophic
1012
1013 573 conditions. Such *in silico* tool provides the opportunity to estimate electron fluxes and their
1014
1015 574 dynamics in the transport chain by using several sets of data including reaction stoichiometry,
1016
1017 575 flux rates, kinetic and thermodynamic constraints. A photosynthesis model of the main electron
1018
1019 576 flow chain reactions consisting of around 50 ordinary differential equations was thereafter
1020
1021 577 developed. It allows to calculate the time depending response of the photosynthetic electron
1022
1023 578 chain to varying light or ambient conditions, allowing a better understanding of several
1024
1025 579 processes such as respiration, carbon fixation or hydrogen production. One interesting result
1026
1027 580 of the model was the description of the thermodynamic mechanism by which, under normal

1021
1022
1023
1024
1025
1026
1027
1028
1029
1030
1031
1032
1033
1034
1035
1036
1037
1038
1039
1040
1041
1042
1043
1044
1045
1046
1047
1048
1049
1050
1051
1052
1053
1054
1055
1056
1057
1058
1059
1060
1061
1062
1063
1064
1065
1066
1067
1068
1069
1070
1071
1072
1073
1074
1075
1076
1077
1078
1079
1080

581 conditions, NADPH acts as an electron acceptor rather than a donor, explaining why it is not
582 possible to sustainably generate such gas in the wild-type strain in normal conditions. Besides,
583 oxygen at cytoplasmic concentrations blocks the hydrogenase activity and moreover, inhibitory
584 levels of oxygen can be reached within seconds after the onset of light. Interestingly, these
585 conditions were numerically confirmed by the model giving not just a qualitatively well-known
586 description of the phenomenon but also shedding light on the process by means of quantitative
587 predictions expressed in physical units.

588
589 Another objective achieved consisted of creating a photobioreactor scale model that is able to
590 predict physiological properties of photosynthetic cultures. Cells grown in such reactors
591 experience complex events: irregular trajectories, inhomogeneity of dissolved carbon and salt
592 concentrations, shear and light stress, among others. However, if cells are grown with an
593 appropriate culture medium and are mixed in a homogeneous and random manner, it can be
594 assumed that they are constantly moving from the reactor surface to the interior part of the
595 vessel. Further, in dense cultures light is not normally leading to photoinhibition but is a
596 limiting variable. In such cases, which are typical for large-scale photobioreactor facilities, it
597 is reasonable to assume that there are two main factors to consider for optimal photosynthesis
598 yields: light as energy input and CO₂ as carbon source. Additionally, in most of the studies
599 performed on photosynthesis research, the Photosynthetically Active Radiation (PAR) value is
600 indicated as reference input for the experiment. Though this is a practical way to show the
601 influence of light on the studied biological mechanism, it does not allow a proper
602 benchmarking with analogous experiments. This is due to the fact that not just the total incident
603 light intensity but also the lamp emission characteristics, the cell concentration, the shape, the
604 depth of the reactor and its previous photoacclimation (Lea-Smith et al., 2014) affect the real
605 irradiance inside the culture vessel and henceforth photosynthesis, too. In addition, all
606 photosynthetic processes are directly regulated by certain wavelengths: pigment light
607 absorption, non-photochemical quenching or state transitions among other mechanisms are
608 controlled by the spectral composition of light and consequently treating light as a simple value
609 is not sufficient for unravelling the underlying mechanisms that control photosynthetic
610 responses. For all these reasons, it was decided to apply the Inherent Optical Properties
611 methodology to predict light quantity and quality in the cell suspension. The model (Fuente et
612 al., 2017), using experimental optical properties validated with literature data of wild-type and
613 Olive strain, delivers reliable results on PAR and spectral light attenuation at different cell
614 densities and LED lamps of several colors. It was later updated with fractional calculus to

1081
1082
1083
1084
1085
1086
1087
1088
1089
1090
1091
1092
1093
1094
1095
1096
1097
1098
1099
1100
1101
1102
1103
1104
1105
1106
1107
1108
1109
1110
1111
1112
1113
1114
1115
1116
1117
1118
1119
1120
1121
1122
1123
1124
1125
1126
1127
1128
1129
1130
1131
1132
1133
1134
1135
1136
1137
1138
1139
1140

615 improve prediction at very depleted light conditions (Fuente, Lizama, Urchueguía, & Conejero,
616 2018). Finally, the light model was coupled with CO₂ gas-liquid mass transfer and
617 cyanobacterial carbon fixation and concentration mechanisms to build up a simplified PBR
618 model that predicts growth with light and carbon as main variables.

619
620 Future *in silico* work will seek the integration of detailed photosynthesis mechanisms as input
621 to genome-scale metabolic models in order to further restrict the solution space towards more
622 realistic metabolic landscapes. Specifically, the effect of light on cells, the so called
623 photoacclimation processes, not yet included in most modelling approaches could be covered
624 in a culture level approach. The final aim is of this analysis is to predict the physiological
625 evolution of main metabolic reporters, understand the resource allocation at any moment of the
626 day and hence suggest operation guidelines for improving overall culture performance.

627 628 **8. Production of flat panel photobioreactors for an industrial standard**

629
630 One key factor for a successful solar biofuel production is the development of an economically
631 feasible PBR production system. Much attention has been given to closed PBRs. Although the
632 setup costs of PBRs are significantly higher than for open ponds, they provide several
633 advantages such as reduced water and CO₂ consumption as well as maintaining unilagal
634 cultures (Schenk et al., 2008). However, closed PBR designs for algal mass cultivation which
635 operate properly and are economically viable are rather scarce (Weissman, Goebel, &
636 Benemann, 1988). Major costs drivers for PBRs are material and manufacturing costs as well
637 as personnel costs (Meyer & Weiss, 2014). Thus, the main focus was on developing a low-cost
638 PBR and an online control system to automate the process of cultivation.

639
640 A flat panel PBR design was chosen since it allows a better exposure to light. To avoid material
641 incompatibility 18 different polymers were tested. To determine the biocompatibility, the
642 optical density (OD) of the samples was determined after 100h, 250h and 400h. The results
643 show that OD increases in all tested samples. Since polymers do not seem to harm algae growth,
644 we used these materials to construct our PBR. Most of the reactor parts can be produced by
645 milling, which allows lower construction costs in comparison to handmade or other saleable
646 versions. The reactors are equipped with industrial standard connectors (G1/8", G1/4", Luer
647 Lock) to ensure adaptability for various applications.

1141
1142
1143
1144
1145
1146
1147
1148
1149
1150
1151
1152
1153
1154
1155
1156
1157
1158
1159
1160
1161
1162
1163
1164
1165
1166
1167
1168
1169
1170
1171
1172
1173
1174
1175
1176
1177
1178
1179
1180
1181
1182
1183
1184
1185
1186
1187
1188
1189
1190
1191
1192
1193
1194
1195
1196
1197
1198
1199
1200

649 To further reduce the setup costs for cultivation in PBRs, a new chemical reactor sterilization
650 process was developed using organic acid to neutralize the peroxide solution. After chemical
651 sterilization, a neutralizing solution is added, which remains in the reactor. This process is
652 especially suitable for large-scale reactors since no further rinsing processes or additional
653 sterilised water is needed. The nutrient solution and culture medium is then added directly to
654 the solution. This process is environmentally less harmful than the previously used EDTA.

655
656 To automate the process of cultivation, an online control system was developed. The program
657 is designed to be freely adjustable to various application setups. Signals can be read by and
658 sent to different ports of the operating computer. Two PCI-Cards for digital in- and output were
659 installed. Thus, different parameters are measured and stored during the cultivation and several
660 actors (valves, pumps, etc) are controlled corresponding to these parameters or to user settings.
661 This enables an online control of the reactor for a user-defined period of time. One advantage
662 of this control system is the possibility of a continuous cultivation without the need of manually
663 adjusting parameters like pH or media flow. This make it possible to keep the culture in a
664 constant state (e.g. constant growth rate) which facilitates reproducible experiments.

665
666 Since water scarcity due to climate change and population growth is gaining in significance,
667 much attention has been paid to the possibility of a closed-loop-system, to ensure a cost
668 effective and resource saving operation. Since photosynthetic microorganisms typically have
669 high water content and harvesting as well as processing requires its removal, it is advantageous
670 to recirculate the extracted water. Thus, the establishment of a simple and low-cost process to
671 separate cyanobacterial biomass from the medium was necessary. Different methods for the
672 separation of the clear phase and the biomass were tested. These include precipitation,
673 electrolysis, and ultrasonic sound. Whereas electrolysis and ultrasonic sound had little or no
674 effect, we found some precipitation agents which lead to a complete separation of solid and
675 liquid phase depending on the type of algae. Problems occurred when we tested the
676 precipitation agent in salty solution. No separation appeared regardless of the amount and type
677 of agent used. Thus, precipitation is a simple and inexpensive filtering for non-salty solutions.

678
679 To operate a closed-loop-system it was essential to test if the separated clear phase leads to
680 precipitation when recirculated to the PBR. During the experiments no precipitation reaction
681 occurred after the recirculation of the chemically sterilized clear phase. Likewise, the second
682 recirculation test after 1 week showed no new precipitation, Figure 10.

1201
1202
1203
1204
1205
1206
1207
1208
1209
1210
1211
1212
1213
1214
1215
1216
1217
1218
1219
1220
1221
1222
1223
1224
1225
1226
1227
1228
1229
1230
1231
1232
1233
1234
1235
1236
1237
1238
1239
1240
1241
1242
1243
1244
1245
1246
1247
1248
1249
1250
1251
1252
1253
1254
1255
1256
1257
1258
1259
1260

683
684
685
686
687
688
689

Another aspect that needs further research is nutrient consumption. This is especially important when the clear phase is recirculated. To save resources and costs it is necessary to investigate if all components of the nutrient solution need to be added after operation, precipitation and filtration. Our test showed that potassium and phosphate have to be added after recirculation with almost no change in iron and zinc after the operation.

9. Assembly and performance assessment of a larger prototype photobioreactor system

690
691
692
693
694
695
696
697
698

A novel flat panel PBR was designed and tested which allowed to reach a light dilution factor close to 4, thus reducing the light saturation effect. The reactor performance has been assessed with a culture of *Synechocystis* 6803, which is a promising candidate for production of biofuels (Touloupakis, Benavides, Cicchi, & Torzillo, 2016a; Touloupakis et al., 2016c). The first attempt to scale up the hydrogen production process with *Synechocystis* 6803, using an indirect light driven process is also reported.

699
700
701
702
703
704
705
706
707
708
709
710
711
712
713

The PBR system (working volume of 1350 L) is composed of 20 vertical parallel plates, each of 50L in volume measuring 1150×1150×50 mm (W×H×D), in direct communication with each other (Figure 11). The inlet of the culture was achieved from the bottom part of each plate through two manifolds (i.d. 9 cm), while the outlet by two manifolds located in the upper part of the plates through which the culture flows back to the degasser. Both the inlet and outlet culture manifolds were constructed with transparent Plexiglas®, therefore, the culture circulates in a parallel mode (i.e. parallel independent compartments). With this type of circulation, the mixing time (T_{mix}) is reduced to about 2 min, which strongly facilitated pH control, CO₂ and nutrient supply, and O₂ degassing of the culture. The plate frames were initially made from PVC, which proved to be inadequate to cope with the temperature stress (up to 70-80 °C in summer, and below zero in winter). Therefore, new replacement ones were made from stainless steel. On top of each plate, there are 4 ports for accessing the culture (i.e., culture sampling, pH, temperature, oxygen probes). The glass windows of the PBR (1150×1150 mm) were made from tempered glass and fixed onto the frame with 32 metal screws (10 mm diameter).

714
715
716

The PBR design was the result of a cooperation between CNR-ISE and M2M Engineering (Naples, IT) who also constructed the PBR. It was installed near the CNR experimental area of

1261
1262
1263 717 Sesto Fiorentino (Firenze), latitude 43.8° N, longitude 11.2° E, and was inoculated with a
1264 718 *Synechocystis* 6803 culture at a concentration of 0.31g/L (DW), maintained at constant
1265 719 temperature of 28°C during the light period and 20-22°C at night (Figure 11). The experiments
1266 720 were carried out with the plates placed at a distance of 0.5 m from each other. The culture
1267 721 behavior was monitored through measurements of chlorophyll fluorescence and dry weight.
1271 722
1272
1273 723 One major problems that occurred during the mass cultivation of *Synechocystis* was the
1274 724 contamination by a flagellate belonging to the species of *Poterioochromonas* (Synurophyceae).
1275 725 It is a very efficient phagotroph, with high growth rates, and *Synechocystis* represented its
1276 726 feeding prey. However, culturing *Synechocystis* at a pH above 11 proved to be a useful strategy
1277 727 to control the contamination with little effect on both culture productivity (less than 10%
1278 728 reduction) and biochemical composition of the biomass (Touloupakis, Cicchi, Benavides, &
1282 729 Torzillo, 2016b).
1283 730
1284 731 The time course of the maximum quantum yield of PSII, F_v/F_m , of the cultures grown in the
1285 732 PBR is show in Figure 11. The maximum F_v/F_m ratio decreased at noon to 72.2% of the initial
1286 733 morning value, indicating that the cultures were subject to photoinhibition, despite the high
1287 734 ratio between illuminated area and ground area occupied the reactor which should allow a
1288 735 reduction of the light intensity on the plates (AR/AG) (Figure 11). Indeed, portions of the plates
1289 736 were still exposed to high light (above 1000 $\mu\text{mol photons m}^{-2} \text{s}^{-1}$). The productivity of the
1290 737 culture was 185 $\text{mg L}^{-1} \text{day}$. The protein content of the biomass grown in the PBR decreased
1291 738 as carbohydrates content increased (Table 3).
1292 739
1293
1294
1295
1296
1297
1298
1299
1300 740 Outdoor hydrogen production experiments were carried out in a 50 L tubular PBR according
1301 741 to an indirect biophotolysis process. The PBR was inoculated with laboratory grown cultures
1302 742 and filled up with BG11₀ medium, obtaining a biomass concentration of 0.36 g L^{-1} and
1303 743 chlorophyll concentration of $7.48 \pm 0.06 \text{ mg L}^{-1}$. Cell growth proceeded until all available
1304 744 nitrate was consumed. During the outdoor experiments, temperature was maintained at $28.0 \pm$
1305 745 $0.5 \text{ }^\circ\text{C}$, with an initial pH of 7.5. *Synechocystis* cells started to accumulate carbohydrates during
1306 746 the day, and usually partially consumed them at night through respiration. At the end of the
1307 747 third day, before the start of the dark anoxic phase, carbohydrate content was $62.5 \pm 0.4\%$ of
1308 748 dry weight while cell biomass concentration had increased from 0.36 ± 0.03 to $0.78 \pm 0.01 \text{ g}$
1309 749 L^{-1} (Figure 12). At the end of the carbohydrate accumulation phase, the cultures were bubbled
1310 750 with N_2 gas and covered with a black sheet to prevent light penetration. Hydrogen release
1311
1312
1313
1314
1315
1316
1317
1318
1319
1320

1321
1322
1323 751 started immediately after degassing for a final total output of 312 mL PBR⁻¹ (i.e. 285 mL in
1324 752 the headspace plus 27 mL dissolved in the culture medium) showing a maximum hydrogen
1326 753 production rate of 0.778 mL H₂ L⁻¹ h⁻¹ (Figure 12). During this phase 0.057 g/L of
1328 754 carbohydrates were fermented (i.e. 2.77 g per reactor).
1329
1330 755

1331 756 Above described study (Touloupakis, Benavides, Cicchi, & Torzillo, 2016a) represents the first
1332 757 attempt to scale up hydrogen production with *Synechocystis* 6803 cells cultivated outdoors
1333 758 under solar illumination, in a 50L tubular PBR. One benefit of the indirect light driven process
1334 759 may come from taking advantage of the natural light/dark cycle, which strongly facilitates the
1335 760 separation of aerobic and anaerobic phases. However, further investigation is necessary to
1336 761 consistently improve the growth and carbohydrate accumulation in *Synechocystis* during the
1337 762 light driven phase, and reduce hydrogen fermentation in the dark anoxic conditions.
1342 763

1344 764 **10. Data management and visualization**

1345 765
1346 766 The CyanoFactory research consortium set the stage for a unifying goal to engineer a
1347 767 cyanobacterium into producing desired bio-molecules. In particular, the partners successfully
1348 768 worked at the interface between experimental and computational biology, which implies
1349 769 different understanding of data. The CyanoFactory KnowledgeBase (CFKB), which is a
1350 770 massive expansion of the WholeCell KB, provides a central data hub for members of the
1351 771 consortium and for disseminating project data to the research community. Thus, it provides
1352 772 ways for an improved collaboration between all partners within the CyanoFactory consortium.
1353 773 All partners were experts in different fields from microbial biotechnology or metabolic
1354 774 modelling, up to synthetic biology. The goal of CFKB was to bridge the gap between bio-
1355 775 engineers and bioinformaticians by providing user-friendly functionalities for working with
1356 776 experimental data and for visualizing and contextualizing it in different ways. Besides
1357 777 experimental data, further data is obtained from other biological databases.
1358 778

1359 779 Life science research is dominated by two conditions: interdisciplinarity and high-throughput.
1360 780 The former leads to highly diverse datasets from a content point of view while high-throughput
1361 781 yields massive amounts of data. Both aspects are reflected by the byte-growth of public bio-
1362 782 databases and the diversity of specialized databases. However, quite often more data leads to
1363 783 less understanding. Driven by the methodology of systems biology, a holistic view of genetic
1364 784 and metabolic regulatory processes is demanded. One important goal is the application of these
1365
1366
1367
1368
1369
1370
1371
1372
1373
1374
1375
1376
1377
1378
1379
1380

1381
1382
1383
1384
1385
1386
1387
1388
1389
1390
1391
1392
1393
1394
1395
1396
1397
1398
1399
1400
1401
1402
1403
1404
1405
1406
1407
1408
1409
1410
1411
1412
1413
1414
1415
1416
1417
1418
1419
1420
1421
1422
1423
1424
1425
1426
1427
1428
1429
1430
1431
1432
1433
1434
1435
1436
1437
1438
1439
1440

785 systemic data for *in silico* modelling of biological processes or, ultimately, biological systems,
786 i.e. cells, tissues, organisms. One step towards this goal was the successful prediction of the
787 phenotype from the genotype in *Mycoplasma genitalium* (Karr et al., 2012). The basis to solve
788 this challenge was a database named WholeCell Knowledge Base (WholeCell KB) (Karr,
789 Sanghvi, Macklin, Arora, & Covert, 2013). It contains experimental results from over 900
790 publications and includes more than 1,900 experimentally observed parameters. Importantly,
791 all data have been validated and curated by scientists.

792
793 Another important manually curated database is Brenda (brenda-enzymes.org), which contains
794 over 1.5 million manually curated enzyme parameters. In contrast, GenBank
795 (ncbi.nlm.nih.gov) contains around 180 million individual and 190 million complete genome
796 shotgun sequences that are partially manually uploaded but not curated.

797
798 With the rising amount of biological data and the increasing capabilities of computer hardware,
799 many attempts have been undertaken to automatically harvest, store, cross-link and provide
800 biological data in databases and databases of databases (i.e. data warehouses) (Kind,
801 Zuchantke, & Wünschiers, 2015). However, automatically generated data collections are of
802 limited value (the common garbage-in garbage-out problem), especially in the context of large
803 scale biological engineering as envisioned by the field of synthetic biology. Here, computer
804 models of biological processes build the fundament to targeted (instead of trial-and-error)
805 genetic engineering.

806
807 CFKB is a productive knowledge base, which handles all the information from our partners.
808 Its advantage is that, besides holding information, it provides different visualization techniques
809 and cross-links to other data sources. Uploading of experimental data is supported in different
810 formats. The warehouse provides import functionality for FASTA, GenBank and System
811 Biology Markup Language (SBML). The import runs as a background job and is automatically
812 merged into the current dataset upon completion. All modifications to the knowledge base are
813 logged, therefore changes to all items can be retrieved and rolled back if necessary. Exports
814 are possible in the import formats and furthermore in machine readable XML or JSON formats.
815 The access to individual resources can be restricted by using permissions.

816
817 Besides the hierarchical view of the warehouse the user can group selected data in so called
818 "baskets". A user can create different baskets and group relevant items in them. The general

1441
1442
1443
1444
1445
1446
1447
1448
1449
1450
1451
1452
1453
1454
1455
1456
1457
1458
1459
1460
1461
1462
1463
1464
1465
1466
1467
1468
1469
1470
1471
1472
1473
1474
1475
1476
1477
1478
1479
1480
1481
1482
1483
1484
1485
1486
1487
1488
1489
1490
1491
1492
1493
1494
1495
1496
1497
1498
1499
1500

819 structure of the organism is visualized by using a chromosome viewer. The viewer is fully
820 interactive and provides filtering functionalities. Additional metadata is displayed beneath the
821 genes.

822
823 Metabolic processes and interactions of biochemical components are visualized using the
824 *Process Description Language* of the Systems Biology Graphical Notation (SBGN) (Le
825 Novere et al., 2009). SBGN represents the metabolic model of the organism in a way detailed
826 enough for biochemists and is machine readable, therefore supporting mathematical
827 simulations inside the model. It should, however, be noted that SBGN proved to be confusing
828 to the human eye. Thus, traditional visualizations such as Boehringer Pathway Maps (Marcus,
829 Altman-Gueta, Wolff, & Gurevitz, 2011) or KEGG maps (Kanehisa et al., 2014) may be
830 preferred.

831
832 Metabolic modelling is provided as part of a CyanoDesign plug-in. Flux balance analysis
833 (FBA) is used for the reconstruction of metabolic networks of organisms. A metabolic network
834 consists of multiple enzymatic reactions with metabolites contained in a stoichiometric matrix
835 (positive for production, negative for degradation). This network is solved using a linear
836 solving method. The motivation behind CyanoDesign is allowing the bio-engineer to change
837 the metabolic network *in silico* and to get a prediction, how the organism is likely to behave.
838 A modelling approach saves valuable time because it gives hints how mutants of the organism
839 may behave, resulting in a high amount of saved work in the lab. FBA is done using the library
840 PyNetMet (Gamermann et al., 2011) and for improved quality of the simulation results the
841 addition of more advanced algorithms like "Minimization of Metabolic Adjustment" (MOMA)
842 can be used.

843 844 845 **Acknowledgement**

846
847 The collaborate research discussed above received funding from the European Union Seventh
848 Framework Programme (FP7/2007-2013) under the grant agreement number 308518 (project
849 CyanoFactory).

850 851 852 **References**

853
854 Altelaar, A. F. M., Frese, C. K., Preisinger, C., Hennrich, M. L., Schram, A. W., Timmers, H.
855 T. M., Heck, M. & Mohammed, S. (2013). Benchmarking stable isotope labeling based
856 quantitative proteomics. *Journal of Proteomics*, 88, 14–26.

1501
1502
1503 857 <https://doi.org/10.1016/j.jprot.2012.10.009>
1504 858 Baebprasert, W., Jantaro, S., Khetkorn, W., Lindblad, P., & Incharoensakdi, A. (2011).
1505 859 Increased H₂ production in the cyanobacterium *Synechocystis* sp. strain PCC 6803 by
1506 860 redirecting the electron supply via genetic engineering of the nitrate assimilation
1507 861 pathway. *Metabolic Engineering*, 13(5), 610–616.
1508 862 <https://doi.org/10.1016/j.ymben.2011.07.004>
1510 863 Brunk, E., George, K. W., Alonso-Gutierrez, J., Thompson, M., Baidoo, E., Wang, G.,
1511 864 Petzold, C. J., McCloskey, D., Monk, J., Yang, L., O'Brien, E. J., Batth, T. S., Martin,
1512 865 H.G., Feist, A., Adams, P. D., Keasling, J. D., Palsson, B. O., & Lee, T.S. (2016).
1513 866 Characterizing strain variation in engineered *E. coli* using a multi-omics-based
1514 867 workflow. *Cell Systems*, 2(5), 335–346. <https://doi.org/10.1016/j.cels.2016.04.004>
1515 868 Cardinale, S., & Arkin, A. P. (2012). Contextualizing context for synthetic biology -
1516 869 identifying causes of failure of synthetic biological systems. *Biotechnology Journal*,
1517 870 7(7), 856–866. <https://doi.org/10.1002/biot.201200085>
1518 871 Čelešnik, H., Tanšek, A., Tahirović, A., Vižintin, A., Mustar, J., Vidmar, V., & Dolinar, M.
1519 872 (2016). Biosafety of biotechnologically important microalgae: intrinsic suicide switch
1520 873 implementation in cyanobacterium *Synechocystis* sp. PCC 6803. *Biology Open*, 5(4),
1521 874 519–528. <https://doi.org/10.1242/bio.017129>
1522 875 Ferreira, E.A., Pacheco, C.C., Pinto, F., Pereira, J., Lamosa, P., Oliveira, P., Kirov, B.,
1523 876 Jaramillo, A., & Tamagnini, P. (2018). Expanding the toolbox for *Synechocystis* sp.
1524 877 PCC 6803: Characterization of a set of novel promoters and validation of replicative
1525 878 vectors. *Synthetic Biology*, 3(1): ysy014. <https://doi.org/10.1093/synbio/ysy014>
1527 879 Fuente, D., Keller, J., Conejero, J. A., Rögner, M., Rexroth, S., & Urchueguía, J. F. (2017).
1528 880 Light distribution and spectral composition within cultures of micro-algae: Quantitative
1529 881 modelling of the light field in photobioreactors. *Algal Research*, 23, 166–177.
1530 882 <https://doi.org/10.1016/j.algal.2017.01.004>
1531 883 Fuente, D., Lizama, C., Urchueguía, J. F., & Conejero, J. A. (2018). Estimation of the light
1532 884 field inside photosynthetic microorganism cultures through Mittag-Leffler functions at
1533 885 depleted light conditions. *Journal of Quantitative Spectroscopy and Radiative Transfer*,
1534 886 204 (Supplement C), 23–26. <https://doi.org/https://doi.org/10.1016/j.jqsrt.2017.08.012>
1535 887 Gamermann, D., Montagud Aquino, A., Infante, R. J., Triana, J., Urchueguía, J. F., & de
1536 888 Córdoba Castellá, P. J. (2011). PyNetMet: python tools for efficient work with networks
1537 889 and metabolic models. *Computational and Mathematical Biology*, 3(5), 11.
1538 890 <https://doi.org/10183/103727>
1540 891 Gutthann, F., Egert, M., Marques, A., & Appel, J. (2007). Inhibition of respiration and nitrate
1541 892 assimilation enhances photohydrogen evolution under low oxygen concentrations in
1542 893 *Synechocystis* sp. PCC 6803. *Biochimica et Biophysica Acta (BBA)-Bioenergetics*,
1543 894 1767(2), 161–169. <https://doi.org/10.1016/j.bbabi.2006.12.003>
1544 895 Heidorn, T., Camsund, D., Huang, H.-H., Lindberg, P., Oliveira, P., Stensjö, K., & Lindblad,
1545 896 P. (2011). Synthetic biology in cyanobacteria engineering and analyzing novel
1546 897 functions. *Methods in Enzymology*, 497, 539–579. [http://www.doi.org/10.1016/B978-0-](http://www.doi.org/10.1016/B978-0-12-385075-1.00024-X)
1547 898 [12-385075-1.00024-X](http://www.doi.org/10.1016/B978-0-12-385075-1.00024-X)
1548 899 Huang, H.-H., Camsund, D., Lindblad, P., & Heidorn, T. (2010). Design and characterization
1549 900 of molecular tools for a Synthetic Biology approach towards developing cyanobacterial
1550 901 biotechnology. *Nucleic Acids Research*, 38(8), 2577–2593.
1551 902 <https://doi.org/10.1093/nar/gkq164>
1552 903 Imashimizu, M., Bernát, G., Sunamura, E.-I., Broekmans, M., Konno, H., Isato, K., ...
1553 904 Hisabori, T. (2011). Regulation of F₀F₁-ATPase from *Synechocystis* sp. PCC 6803 by γ
1554 905 and δ subunits is significant for light/dark adaptation. *Journal of Biological Chemistry*,
1555 906 286(30), 26595–26602. <http://doi.org/10.1074/jbc.M111.234138>

1561
1562
1563 907 Kalb, V. F., & Bernlohr, R. W. (1977). A new spectrophotometric assay for protein in cell
1564 908 extracts. *Analytical Biochemistry*, 82(2), 362–371. <https://doi.org/10.1016/0003->
1565 909 2697(77)90173-7
1566 910 Kanehisa, M., Goto, S., Sato, Y., Kawashima, M., Furumichi, M., & Tanabe, M. (2014).
1567 911 Data, information, knowledge and principle: back to metabolism in KEGG. *Nucleic*
1568 912 *Acids Research*, 42(D1), D199-D205. <https://dx.doi.org/10.1093/nar/gkt1076>
1570 913 Karr, J. R., Sanghvi, J. C., Macklin, D. N., Arora, A., & Covert, M. W. (2013).
1571 914 WholeCellKB: model organism databases for comprehensive whole-cell models.
1572 915 *Nucleic Acids Research*, 41(D1), D787--D792. <https://dx.doi.org/10.1093/nar/gks1108>
1573 916 Karr, J. R., Sanghvi, J. C., Macklin, D. N., Gutschow, M. V, Jacobs, J. M., Bolival, B., ...
1574 917 Covert, M. W. (2012). A whole-cell computational model predicts phenotype from
1575 918 genotype. *Cell*, 150(2), 389–401. <http://doi.org/10.1016/j.cell.2012.05.044>
1576 919 Kind, G., Zuchantke, E., & Wünschiers, R. (2015). CyanoFactory Knowledge Base &
1577 920 Synthetic Biology - A Plea for Human Curated Bio-databases. In *Proceedings of the*
1578 921 *International Conference on Bioinformatics Models, Methods and Algorithms - Volume*
1579 922 *1: BIOINFORMATICS, (BIOSTEC 2015)* (pp. 237–242). SciTePress.
1580 923 <https://doi.org/10.5220/0005285802370242>
1581 924 Kopfmann, S., Roesch, S. K., & Hess, W. R. (2016). Type II Toxin--Antitoxin Systems in the
1582 925 Unicellular Cyanobacterium *Synechocystis* sp. PCC 6803. *Toxins*, 8(7), 228.
1583 926 <https://doi.org/10.3390/toxins8070228>
1584 927 Kwon, J.-H., Bernát, G., Wagner, H., Rögner, M., & Rexroth, S. (2013). Reduced light-
1585 928 harvesting antenna: Consequences on cyanobacterial metabolism and photosynthetic
1586 929 productivity. *Algal Research*, 2, 188–195. <https://doi.org/10.1016/j.algal.2013.04.008>
1588 930 Landels, A., Evans, C., Noirel, J., & Wright, P. C. (2015). Advances in proteomics for
1589 931 production strain analysis. *Current Opinion in Biotechnology*, 35, 111–117.
1590 932 <https://doi.org/10.1016/j.copbio.2015.05.001>
1591 933 Lea-Smith, D. J., Bombelli, P., Dennis, J. S., Scott, S. A., Smith, A. G., & Howe, C. J.
1592 934 (2014). Phycobilisome-deficient strains of *Synechocystis* sp. PCC 6803 have reduced
1593 935 size and require carbon-limiting conditions to exhibit enhanced productivity. *Plant*
1594 936 *Physiology*, 165, 705–714. <https://doi.org/10.1104/pp.114.237206>
1595 937 Le Novère, N., Hucka M., Mi, H., Moodie, S., Schreiber, F., Sorokin, A., Demir, E., Wegner,
1596 938 K., Aladjem, M. I., Wimalaratne, S. M., Bergman, F. T, Gauges, R., Ghazal, P., Kawaji,
1597 939 H., Li, L., Matsuoka, Y., Villéger, A., Boyd, S. E, Calzone, L., Courtot, M., Dogrusoz,
1598 940 U., Freeman, T. C., Funahashi, A., Ghosh, S., Jouraku, A., Kim, S., Kolpakov, F., Luna,
1599 941 A., Sahle, S., Schmidt, E., Watterson, S., Wu, G., Goryanin, I., Kell, D. B., Sander, C.,
1600 942 Sauro, H., Snoep, J. L., Kohn K., & Kitano, H. (2009). The systems biology graphical
1601 943 notation. *Nature Biotechnology*, 27(8), 735–741. <http://doi.org/10.1038/nbt.1558>
1603 944 Liauw, P., Mashiba, T., Kopczak, M., Wiegand, K., Muraki, N., Kubota, H., Kawano, Y.,
1604 945 Ikeuchi, M., Hase, T., Rögner, M., Kurisu, G. (2012). Cloning, expression,
1605 946 crystallization and preliminary X-ray studies of the ferredoxin-NAD(P)⁺ reductase from
1606 947 the thermophilic cyanobacterium *Thermosynechococcus elongatus* BP-1. *Acta*
1607 948 *Crystallographica Section F: Structural Biology and Crystallization Communications*,
1608 949 68(9), 1048–1051. <http://doi.org/10.1107/S1744309112031910>
1609 950 Marcus, Y., Altman-Gueta, H., Wolff, Y., & Gurevitz, M. (2011). Rubisco mutagenesis
1610 951 provides new insight into limitations on photosynthesis and growth in *Synechocystis*
1611 952 PCC6803. *Journal of Experimental Botany*, 62(12), 4173–4182.
1612 953 <https://dx.doi.org/10.1093/jxb/err116>
1613 954 Markley, A. L., Begemann, M. B., Clarke, R. E., Gordon, G. C., & Pflieger, B. F. (2015).
1614 955 Synthetic biology toolbox for controlling gene expression in the cyanobacterium
1615 956 *Synechococcus* sp. strain PCC 7002. *ACS Synthetic Biology*, 4(5), 595–603.

1621
1622
1623 957 <https://doi.org/10.1021/sb500260k>
1624 958 Meyer, M. A., & Weiss, A. (2014). Life cycle costs for the optimized production of hydrogen
1625 959 and biogas from microalgae. *Energy*, 78, 84–93.
1626 960 <https://doi.org/10.1016/j.energy.2014.08.069>
1628 961 Montagud, A., Navarro, E., Fernández de Córdoba, P., Urchueguía, J. F., & Patil, K. R.
1629 962 (2010). Reconstruction and analysis of genome-scale metabolic model of a
1630 963 photosynthetic bacterium. *BMC Systems Biology*, 4(1), 156.
1631 964 <https://doi.org/10.1186/1752-0509-4-156>
1632 965 Montagud, A., Zelezniak, A., Navarro, E., Fernández de Córdoba, P., Urchueguía, J. F., &
1633 966 Patil, K. R. (2011). Flux coupling and transcriptional regulation within the metabolic
1634 967 network of the photosynthetic bacterium *Synechocystis* sp. PCC6803. *Biotechnology*
1635 968 *Journal*, 6(3), 330–42. <https://doi.org/10.1002/biot.201000109>
1636 969 Muro-Pastor, A. M., Flores, E., Herrero, A., & Wolk, C. P. (1992). Identification, genetic
1637 970 analysis and characterization of a sugar-non-specific nuclease from the cyanobacterium
1638 971 *Anabaena* sp. PCC 7120. *Molecular Microbiology*, 6(20), 3021–3030.
1639 972 <https://doi.org/10.1111/j.1365-2958.1992.tb01760.x>
1640 973 Mutalik, V. K., Guimaraes, J. C., Cambray, G., Lam, C., Christoffersen, M. J., Mai, Q.-A.,
1641 974 Tran, A. B., Paull, M., Keasling, J. D., Arkin, A. P., Endy, D. (2013). Precise and
1642 975 reliable gene expression via standard transcription and translation initiation elements.
1643 976 *Nature Methods*, 10(4), 354–360. <http://doi.org/10.1038/nmeth.2404>
1645 977 Oliveira, P., Martins, N. M., Santos, M., Pinto, F., Büttel, Z., Couto, N. A. S., Wright, P. C.,
1646 978 & Tamagnini, P. (2016). The versatile TolC-like Slr1270 in the cyanobacterium
1647 979 *Synechocystis* sp. PCC 6803. *Environmental Microbiology*, 18(2), 486–502.
1648 980 <https://doi.org/10.1111/1462-2920.13172>
1649 981 Pacheco, C.C, Büttel, Z., Pinto, F., Rodrigo, G., Carrera, J., Jaramillo, A., & Tamagnini, P.
1650 982 (2018). Modulation of intracellular O₂ concentration in *Escherichia coli* strains using
1651 983 Oxygen Consuming Devices (OCDs). *ACS Synthetic Biology*, 7 (7), 1742–1752.
1652 984 <https://doi.org/10.1021/acssynbio.7b00428>
1653 985 Page, L. E., Liberton, M., & Pakrasi, H. B. (2012). Reduction of photoautotrophic
1654 986 productivity in the cyanobacterium *Synechocystis* sp. strain PCC 6803 by phycobilisome
1655 987 antenna truncation. *Applied and Environmental Microbiology*, 78(17), 6349–6351.
1656 988 <https://doi.org/10.1128/AEM.00499-12>
1657 989 Pinto, F., Pacheco, C. C., Oliveira, P., Montagud, A., Landels, A., Couto, N., Wright, P. C.,
1658 990 Urchueguía, J. F., & Tamagnini, P. (2015). Improving a *Synechocystis*-based
1659 991 photoautotrophic chassis through systematic genome mapping and validation of neutral
1660 992 sites. *DNA Research*, 22(6), 425–437. <https://dx.doi.org/10.1093/dnares/dsv024>
1662 993 Ramey, C. J., Barón-Sola, A., Aucoin, H. R., & Boyle, N. R. (2015). Genome engineering in
1663 994 cyanobacteria: where we are and where we need to go. *ACS Synthetic Biology*, 4(11),
1664 995 1186–1196. <https://doi.org/10.1021/acssynbio.5b00043>
1665 996 Schenk, P. M., Thomas-Hall, S. R., Stephens, E., Marx, U. C., Mussgnug, J. H., Posten, C.,
1666 997 Kruse, O. & Hankamer, B. (2008). Second generation biofuels: high-efficiency
1667 998 microalgae for biodiesel production. *Bioenergy Research*, 1(1), 20–43.
1668 999 <https://doi.org/10.1007/s12155-008-9008-8>
1669 1000 Touloupakis, E., Benavides, A. M. S., Cicchi, B., & Torzillo, G. (2016a). Growth and
1670 1001 hydrogen production of outdoor cultures of *Synechocystis* PCC 6803. *Algal Research*,
1671 1002 18, 78–85. <https://dx.doi.org/10.1016/j.algal.2016.06.010>
1672 1003 Touloupakis, E., Cicchi, B., Benavides, A. M. S., & Torzillo, G. (2016b). Effect of high pH
1673 1004 on growth of *Synechocystis* sp. PCC 6803 cultures and their contamination by golden
1674 1005 algae (*Poteroiochromonas* sp.). *Applied Microbiology and Biotechnology*, 100(3),
1675 1006 1333–1341. <https://doi.org/10.1007/s00253-015-7024-0>
1676
1677
1678
1679
1680

1681
1682
1683
1684
1685
1686
1687
1688
1689
1690
1691
1692
1693
1694
1695
1696
1697
1698
1699
1700
1701
1702
1703
1704
1705
1706
1707
1708
1709
1710
1711
1712
1713
1714
1715
1716
1717
1718
1719
1720
1721
1722
1723
1724
1725
1726
1727
1728
1729
1730
1731
1732
1733
1734
1735
1736
1737
1738
1739
1740

Touloupakis, E., Rontogiannis, G., Benavides, A. M. S., Cicchi, B., Ghanotakis, D. F., & Torzillo, G. (2016c). Hydrogen production by immobilized *Synechocystis* sp. PCC 6803. *International Journal of Hydrogen Energy*, *41*(34), 15181–15186. <https://doi.org/10.1016/j.ijhydene.2016.07.075>

Wegelius, A., Khanna, N., Esmieu, C., Barone, G. D., Pinto, F., Tamagnini, P., Berggren, G., & Lindblad, P. (2018). Generation of a functional, semisynthetic [FeFe]-hydrogenase in a photosynthetic microorganism. *Energy and Environmental Science* *11* (11), 3163-3167. <https://doi.org/10.1039/C8EE01975D>

Weissman, J. C., Goebel, R. P., & Benemann, J. R. (1988). Photobioreactor design: mixing, carbon utilization, and oxygen accumulation. *Biotechnology and Bioengineering*, *31*(4), 336–344. <https://doi.org/10.1002/bit.260310409>

Wiegand et al. 2018 - Wiegand K, Winkler M, Rumpel S, Kannchen D, Rexroth S, Hase T, Farès C, Happe T, Lubitz W, Rögner M (2018). Rational redesign of the ferredoxin-NADP+-oxido-reductase/ferredoxin-interaction for photosynthesis-dependent H₂-production. *Biochim Biophys Acta* *1859*(4):253-262. <https://doi.org/10.1016/j.bbabi.2018.01.006>

Wright, O., Stan, G.-B., & Ellis, T. (2013). Building-in biosafety for synthetic biology. *Microbiology*, *159*(7), 1221–1235. <https://doi.org/10.1099/mic.0.066308-0>

Wünschiers, R. (2016). Making-of Synthetic Biology: The European CyanoFactory Research Consortium. In K. Hagen, Engelhard Margret, & G. Toepfer (Eds.), *Ambivalences of Creating Life: Societal and Philosophical Dimensions of Synthetic Biology* (pp. 55–72). Cham: Springer International Publishing. https://doi.org/10.1007/978-3-319-21088-9_3

Yizhak, K., Benyamini, T., Liebermeister, W., Ruppin, E., & Shlomi, T. (2010). Integrating quantitative proteomics and metabolomics with a genome-scale metabolic network model. *Bioinformatics (Oxford, England)*, *26*(12), i255-260. <https://doi.org/10.1093/bioinformatics/btq183>

Zhou, J., Zhang, H., Meng, H., Zhu, Y., Bao, G., Zhang, Y., Li, Y., & Ma, Y. (2014). Discovery of a super-strong promoter enables efficient production of heterologous proteins in cyanobacteria. *Scientific Reports*, *4*:4500. <https://doi.org/10.1038/srep04500>

Zhou, J., Zhu, T., Cai, Z., & Li, Y. (2016). From cyanochemicals to cyanofactories: a review and perspective. *Microbial Cell Factories*, *15*(1), 2. <https://doi.org/10.1186/s12934-015-0405-3>

Figures, 1 to 12

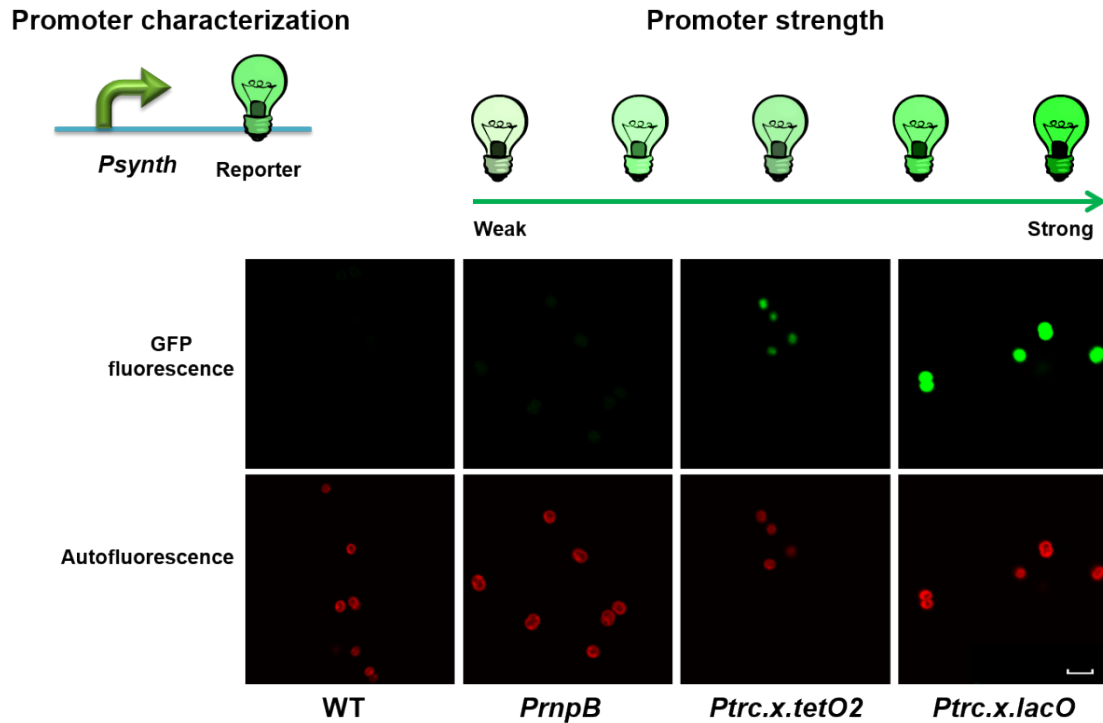


Figure 1. Confocal micrographs of *Synechocystis* wild-type (WT) cells and *Synechocystis* mutant cells harbouring the *PrnpB*, *Ptrc.x.tetO2* or *Ptrc.x.lacO* promoters assembled with a GFP generator. GFP fluorescence is depicted in the top row and the autofluorescence is depicted in the bottom row. Scale bar, 5 μm .

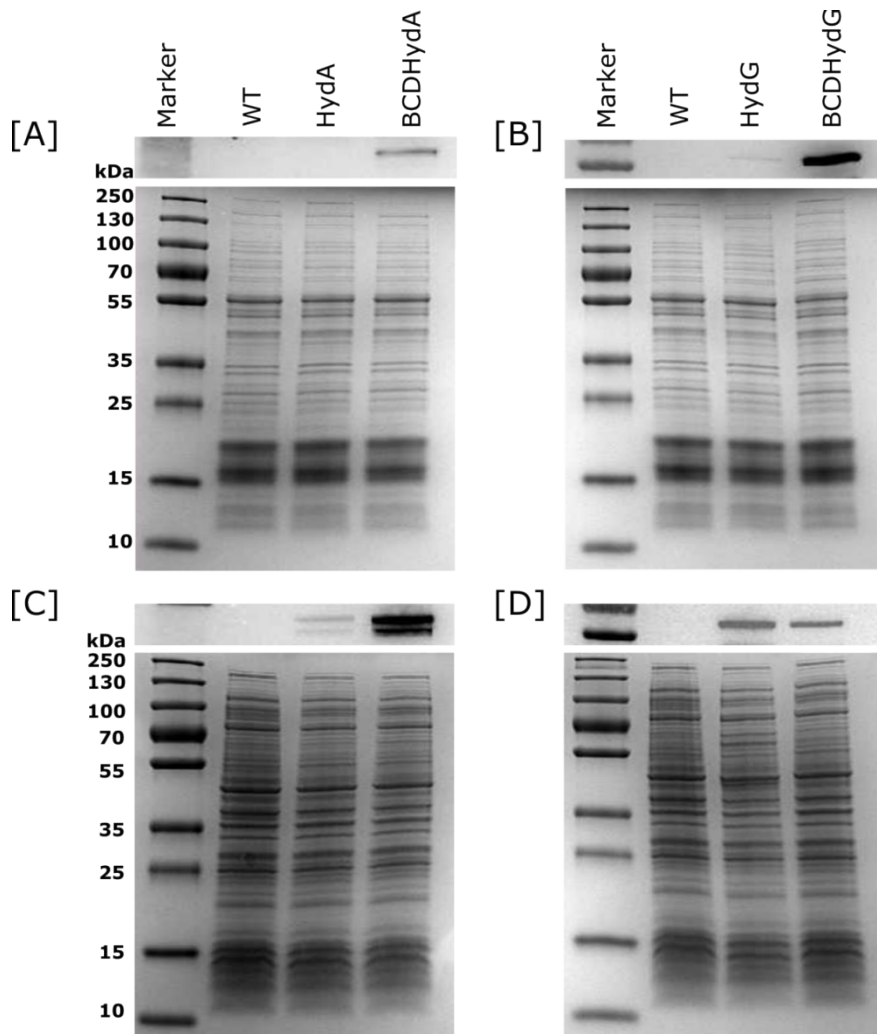


Figure 2. SDS-PAGE and Western immunoblots analysis of crude protein extracts from *Synechocystis* (A, B) and *E. coli* DH5 α (C, D) wild type and engineered strains using HydA antibodies (A, C) and flag tag antibodies (B, D). Proteins from *Synechocystis* were isolated from 25 mL mid-log phase cultures (O.D. = 1.0 ± 0.2) as described in Heidorn et al. (2011). The protein concentrations were determined using colorimetric Bradford protein assay (Bio-Rad Laboratories) and 10 μ g total proteins were loaded in each well. For *E. coli* protein extraction, pre-cultures were grown overnight at 37 °C, 200 rpm shaking, in LB media containing 50 μ g/ml kanamycin, and used to inoculate 20 mL of LB media supplemented with antibiotics and 0.5 mM IPTG. Cultures were grown aerobically at 37 °C for 3 h and thereafter 1 mL of culture was harvested and re-suspended in water as per the O.D. 18 μ L of total proteins were loaded in each well. The proteins were separated on precast (any kD) acrylamide gels (Bio-Rad) run at 200 V. Separated polypeptides were transferred to PVDF membranes (Bio-Rad), probed with (A, C) rabbit-anti-HydA IgG (Agrisera AS09 514) as per the manufacturer's instructions before visualization using goat-anti-rabbit IgG-HRP conjugate (Bio-Rad) and (B, D) with mouse-anti-flag IgG (Sigma F3165) as per the manufacturer's instructions before visualization using goat-anti-mouse IgG-HRP conjugate (Bio-Rad). The secondary antibodies were used at a 1:5000 dilution for 1 h. Detection was performed using Immuno-Star HRP Substrate (Bio-Rad), and recorded using a ChemiDoc XRS system (Bio-Rad).

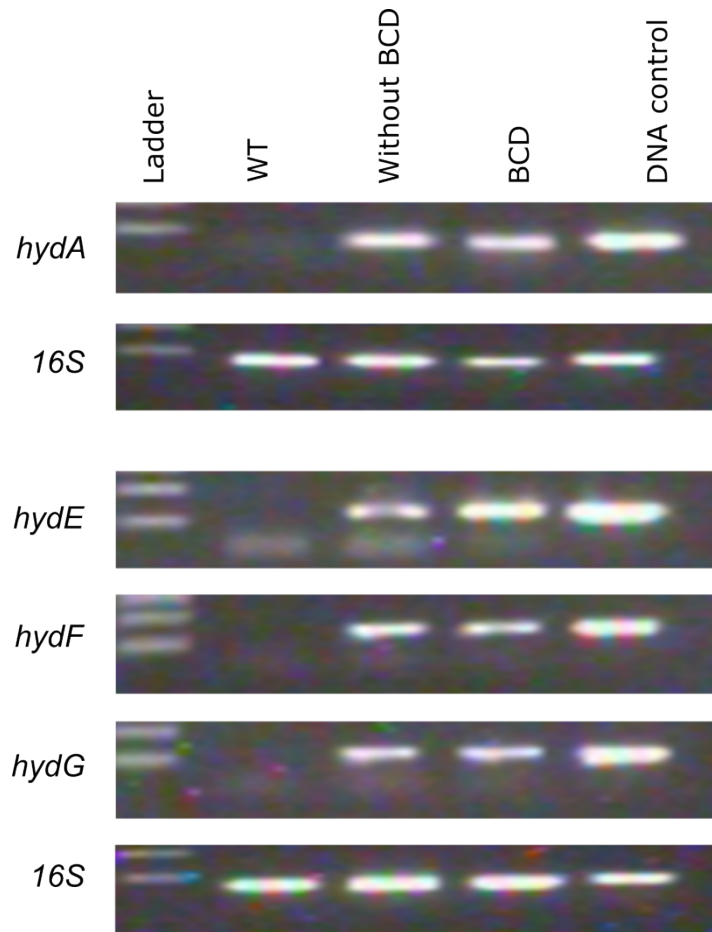


Figure 3. RNA isolated from 10 mL early log-phase *Synechocystis* PCC 6803 wild type and engineered strains (O.D. = 0.4 ± 0.2) as described in Heidorn et al. (2011). 50 ng of plasmid or genomic DNA were used as control. cDNA was prepared as per the manufacturer's instructions (Quanta BIOSCIENCES). 100 ng of the first-strand reaction was used for PCR amplification (28 cycles). PCR amplicons (20 cycles) of 16S rRNA were used as loading control. The primer pair sequences (5' to 3') used in the study were as follows: RTHydA-F: gcaacaaagtgaagctgatcg, RT HydA-R: ctccatgggattatccattc; RTMatE-F: cactgtagagaaaatgaaatataatcg, RTMatE-R: gcatcaattctttaagaacaaaat; RTMatF-F: ctattccctcttattagagaaaaag, RTMatF-R: cgtaattcaaattccttcgtaac; RTMatG-F: caagacatgggtcataaacg, RTMatG-R: gcttcgtagatgacgcat; RT16S-F: cactgggactgagacac RT16S-R: ctgctggcacggagtttag.

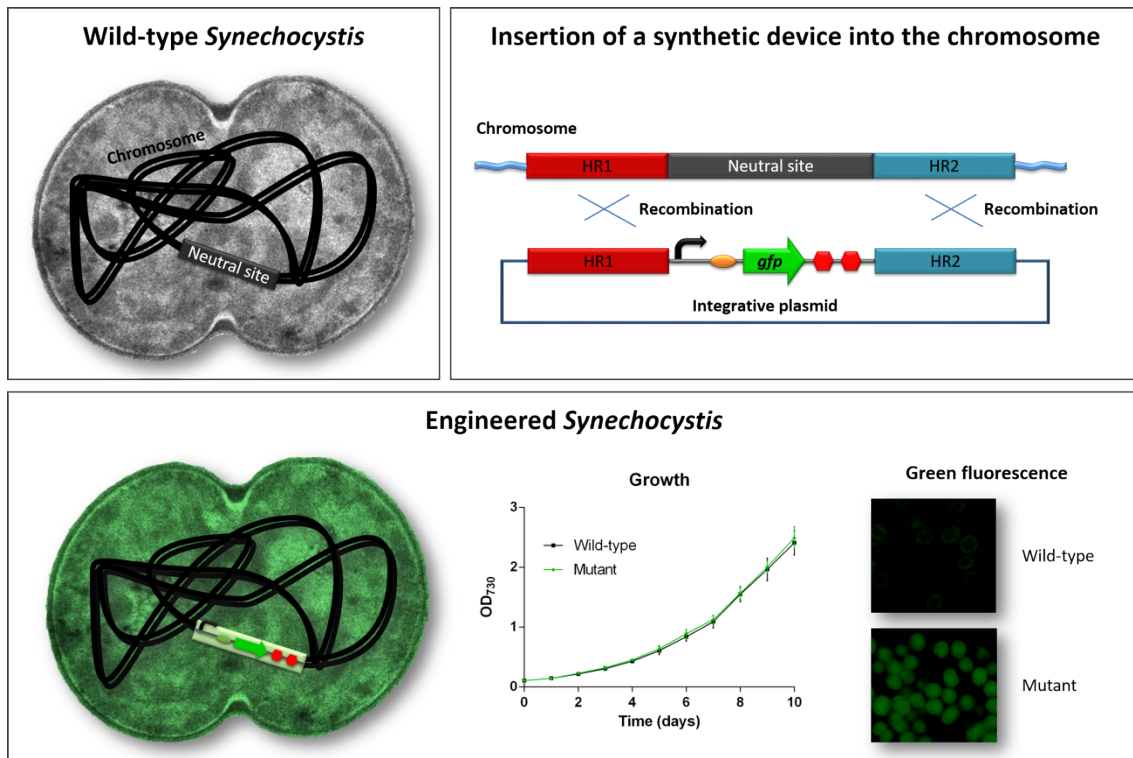


Figure 4. Schematic representation of the methodology employed by Pinto et al. (2015) to validate *Synechocystis* genomic neutral sites. The identified potential genomic neutral site (upper left panel) was modified by the insertion of a synthetic device containing a GFP generator (upper right panel). The neutrality of the putative neutral site was further validated assessing cell fitness, while functionality of the inserted device was analyzed by confocal microscopy (bottom panel).

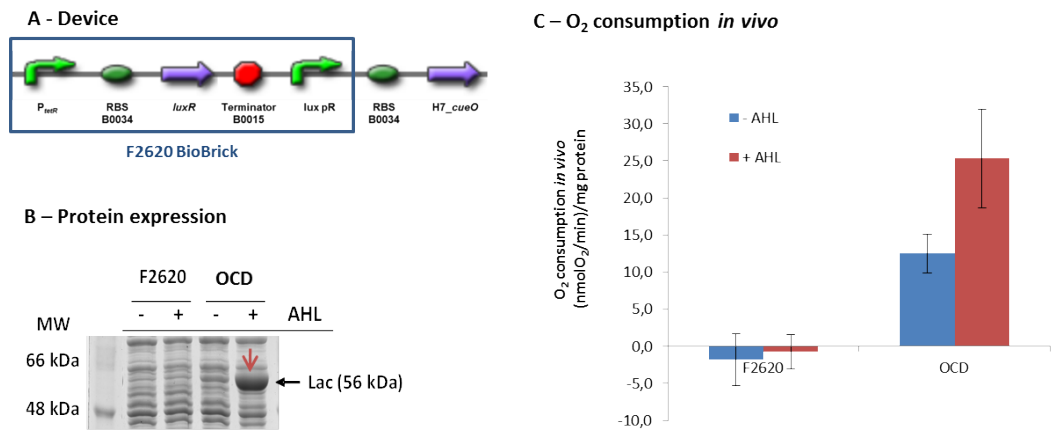


Figure 5. Characterization of *E. coli* Top10 harboring the laccase-based OCD. (A) Specifications of the synthetic device. (B) Analysis of protein expression by SDS-PAGE. Protein extracts were obtained from *E. coli* Top10 containing the F2620 BioBrick or the OCD, in presence (+) or absence (-) of the inducer - AHL. The band corresponding to the laccase is highlighted by a red arrow. (C) O₂ consumption measurements *in vivo*. Cultures from *E. coli* Top10 containing the F2620 or the OCD, in presence (+) or absence (-) of AHL were used; and respiration rates were determined polarographically for suspensions with a final OD₆₀₀=1, 2 or 4 (1 mL working volume) using a Clark-type O₂ electrode. Error bars represent the standard deviation of statistical means of 3 biological replicates.

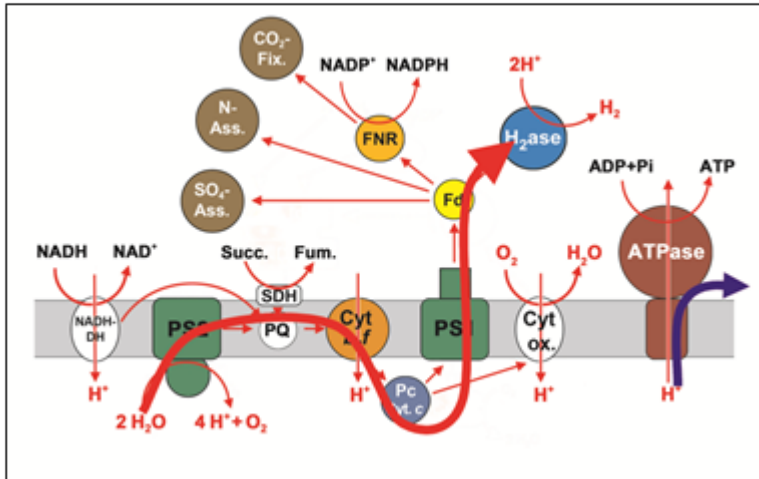


Figure 6. Schematic outline of an optimized electron flow towards the hydrogenase for photosynthetic hydrogen production.

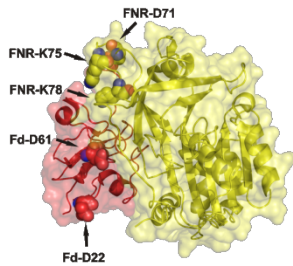


Figure 7. Structure of the FNR:Fd complex. The sites targeted for reducing the complex stability are identified labelled, protein followed by amino acid and its number, within the structure.

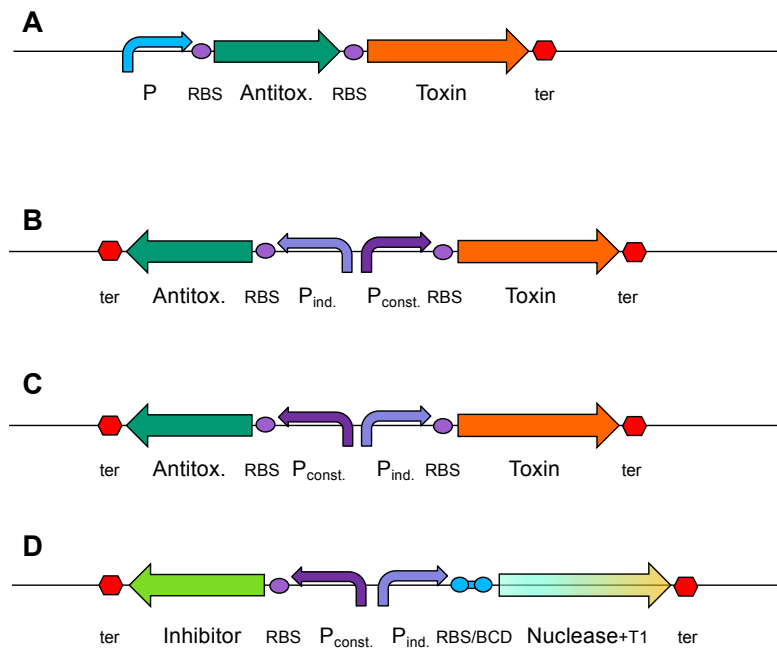


Figure 8. The native TAS (A) and engineered effector/inhibitor device design for controlled cell death (B-D); toxin/antitoxin-based devices (B, C) and the optimized nuclease/inhibitor-based device (D). (A) The native arrangement of the toxin and antitoxin genes under the control of a single common promoter. (B) The engineered arrangement that could be used for induced expression of the antitoxin in the bioreactor. Upon spillage, inducer would no longer be available, resulting in toxin activity and possibly cell death. (C) Alternative engineered arrangement that could be used for induction of the toxin gene at the spill site upon leakage, thus saving costs of continually adding inducer in the bioreactor under regular growth conditions. (D) A variant of (C) with the controlled expression of nuclease/inhibitor; this configuration showed best results in induced cell killing. Abbreviations: Antitox., antitoxin-coding region; BCD, bicistronic design (a specific transition between the RBS and the start codon that promotes reliable translation initiation); P, wild-type promoter; $P_{ind.}$, inducible promoter; $P_{const.}$, constitutive promoter; RBS, ribosome binding site; ter, transcription terminator, T1: degradation tag.

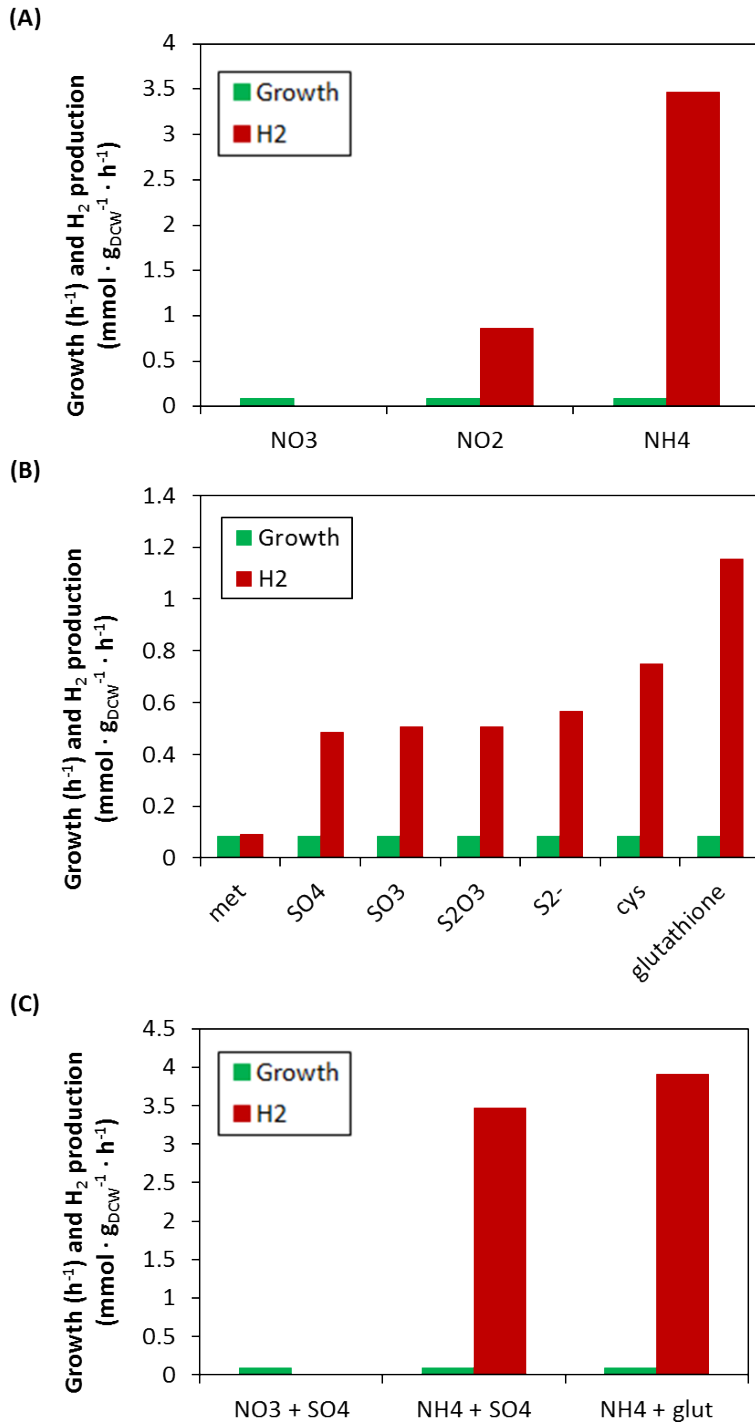


Figure 9. Results of the simulation of hydrogen production at a given growth rate with different sources of inorganic nutrients obtained by using the *Synechocystis* 6803 metabolic model. Simulations were carried out under phototrophic conditions, with fixed amount of photons and CO₂, at a fixed growth ratio (normal growth for this carbon intake), and allowing the input of different (A) nitrogen sources: nitrate (NO₃⁻), nitrite (NO₂⁻) and ammonia (NH₄⁺); (B) sulphur sources: methionine (met), sulphate (SO₄), sulphite (SO₃⁻), thiosulphate (S₂O₃), sulphide (S₂⁻), cysteine (cys) and glutathione; and (C) combination of nitrogen and sulphur sources leading at best maximum optimal hydrogen production.

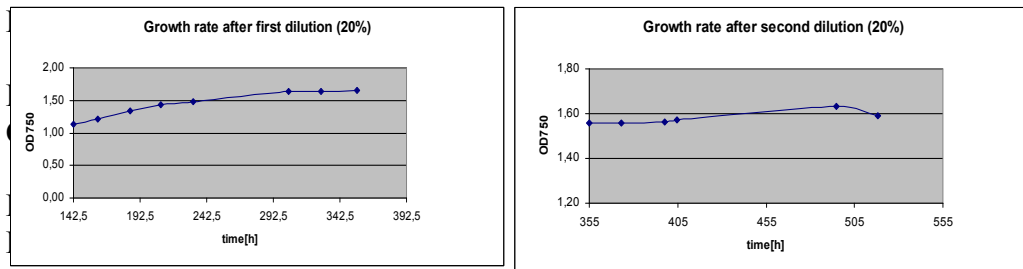


Figure 10. Growth rates after first (left) and second (right) recirculation (dilution) with no observed precipitations.

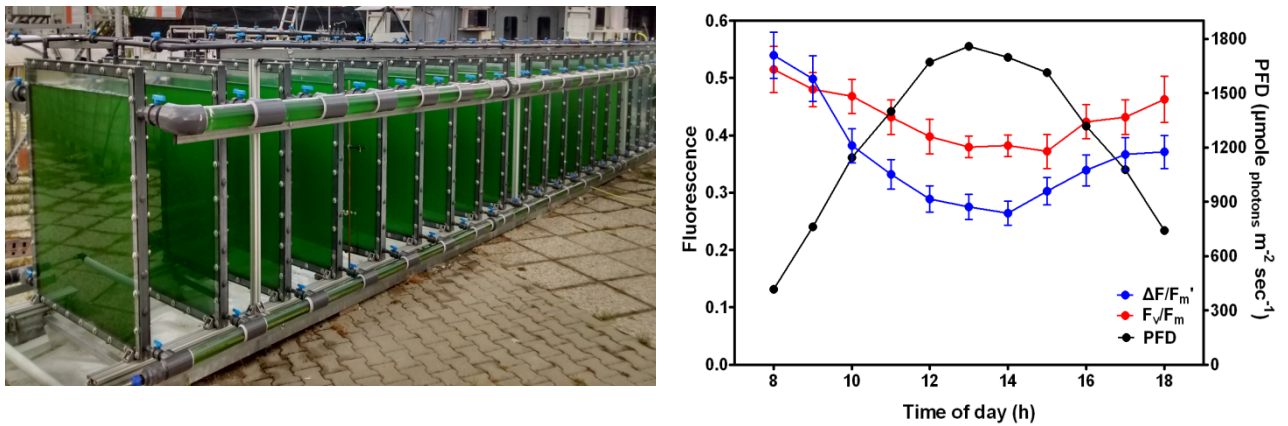


Figure 11. The flat panel PhotoBioReactor (PBR) system (maximum working volume 1300L) is composed of 20 vertical parallel plates 50L, 1150×1150×50mm ($W \times H \times D$), in direct communication with each other, left. Daily variation of maximum quantum efficiency of PSII photochemistry (F_v/F_m) and effective photochemical quantum yield of PSII ($\Delta F/F_m'$) right.

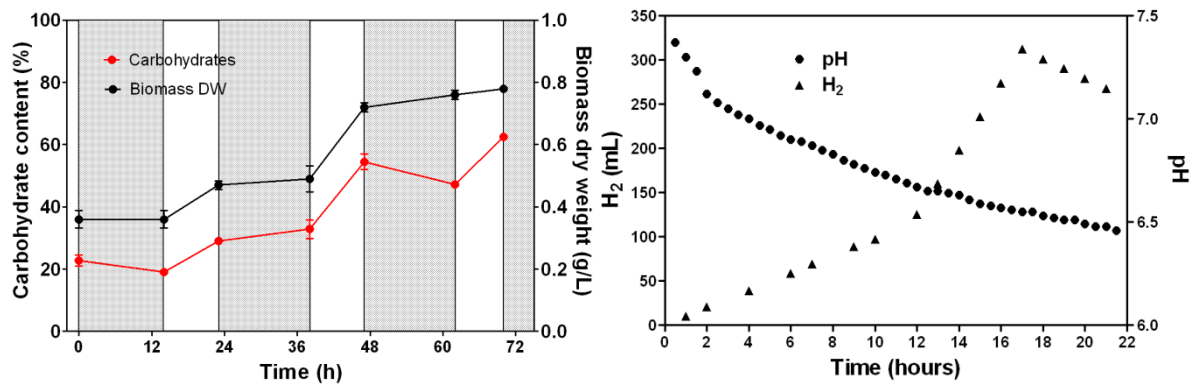


Figure 12. Carbohydrate content and biomass concentration in a *Synechocystis* 6803 cell culture during an outdoor experiment. During the first 72 hours, carbohydrate accumulation take place; at 72 hours, the dark anaerobic/hydrogen production phase starts (day-*white bars*, night-*gray bars*), left. pH value and H₂ (mL) accumulation of the *Synechocystis* cell culture under an dark and anaerobic condition, right.

Tables, 1 to 3

Table 1. List of FNR and Fd variants ordered by decreasing affinity.

| FNR variants | Fd variants |
|-----------------------------|--------------------|
| FNR _{L/S} | Fd |
| FNR _S -D71K | Fd-D22A |
| FNR _S -K75A | Fd-D61A |
| FNR _S -K75D | Fd-D22A-D61A |
| FNR _S -K78A | |
| FNR _S -K78D | |
| FNR _S -K78A-K78D | |
| FNR _S -K75D-K78D | |

Table 2. Synthetic biology devices examined, along with the observed behaviour in the process of cloning and testing. Top: nuclease/inhibitor-based devices; bottom: toxin/antitoxin-based devices. The two best-performing constructs are presented in bold at the top of the list. Promoters, effectors and effector antagonists are explained in the text. T1, T2: degradation tags.

| Promoter – nuclease | | Promoter – nuc. inhibitor | | Switch activity |
|-------------------------------------|-----------------|-------------------------------------|-------------|--|
| <i>copM</i> _{195-BCD} | <i>nucA</i> -T1 | <i>rnpB</i> _{RBS} | <i>nuiA</i> | complete autodestruction upon Zn²⁺ - induction |
| <i>copM</i> ₇₂ | <i>nucA</i> -T1 | <i>rnpB</i> _{RBS} | <i>nuiA</i> | marked autotoxicity upon Zn²⁺ - induction |
| <i>copB</i> | <i>nucA</i> -T2 | <i>rnpB</i> _{RBS} | <i>nuiA</i> | only mutated clones survive |
| <i>rnpB</i> _{RBS} | <i>nucA</i> | <i>copB</i> | <i>nuiA</i> | only mutated clones survive |
| <i>rnpB</i> _{RBS} | <i>nucA</i> -T2 | <i>copB</i> | <i>nuiA</i> | cyanobacterial transformantion failed |
| <i>nrsB</i> _{native} | <i>nucA</i> -T1 | <i>rbcL1A</i> | <i>nuiA</i> | weak autotoxicity |
| <i>nrsB</i> _{RBS} | <i>nucA</i> -T2 | <i>rbcL1A</i> | <i>nuiA</i> | weak autotoxicity |
| <i>nrsB</i> _{BCD} | <i>nucA</i> -T1 | <i>rnpB</i> _{RBS} | <i>nuiA</i> | weak autotoxicity |
| <i>nrsB</i> _{native-short} | <i>nucA</i> -T1 | <i>rbcL1A</i> | <i>nuiA</i> | weak autotoxicity |
| <i>nrsB</i> _{native-short} | <i>nucA</i> -T2 | <i>rbcL1A</i> | <i>nuiA</i> | weak autotoxicity |
| <i>rbcL1A</i> | <i>nucA</i> -T1 | <i>nrsB</i> _{native-short} | <i>nuiA</i> | metal-ion dependent toxicity <i>not</i> observed |
| <i>rbcL1A</i> | <i>nucA</i> -T2 | <i>nrsB</i> _{native-short} | <i>nuiA</i> | metal-ion dependent toxicity <i>not</i> observed |

| Promoter – toxin | | Promoter – antitoxin | | Switch activity |
|----------------------------|----------------|----------------------------|----------------|---|
| <i>smtA</i> | <i>slr0664</i> | <i>rnpB</i> _{RBS} | <i>ssr1114</i> | only mutated clones survive |
| <i>rnpB</i> _{RBS} | <i>slr0664</i> | <i>smtA</i> | <i>ssr1114</i> | weak autotoxicity (Zn ²⁺ or Cu ²⁺ withdrawal) |
| <i>rnpB</i> _{RBS} | <i>slr0664</i> | <i>copB</i> | <i>ssr1114</i> | weak autotoxicity (Zn ²⁺ or Cu ²⁺ withdrawal) |
| <i>copB</i> | <i>slr0664</i> | <i>rnpB</i> _{RBS} | <i>ssr1114</i> | weak autotoxicity upon Zn ²⁺ - induction |
| <i>nrsB</i> _{RBS} | <i>slr0664</i> | <i>rnpB</i> _{RBS} | <i>ssr1114</i> | metal-ion dependent toxicity <i>not</i> observed |

Table 3. Daily variation of biomass (dry weight, DW), protein, carbohydrate and chlorophyll (Chl) contents of a *Synechocystis* 6803 culture in the flat panel PBR. Values are mean \pm standard deviations.

| Daytime | DW (g/L) | Protein (%) | Carbohydrate (%) | Chlorophyll (%) |
|----------------|-------------------|--------------------|-------------------------|------------------------|
| 08:00 | 0.315 \pm 0.007 | 41.49 \pm 0.93 | 12.60 \pm 0.28 | 1.86 \pm 0.09 |
| 10:00 | 0.330 \pm 0.056 | 43.90 \pm 7.52 | 12.95 \pm 2.22 | 1.81 \pm 0.05 |
| 12:00 | 0.340 \pm 0.000 | 46.27 \pm 0.64 | 15.15 \pm 0.27 | 1.91 \pm 0.13 |
| 14:00 | 0.415 \pm 0.007 | 42.12 \pm 0.71 | 16.32 \pm 0.28 | 1.76 \pm 0.09 |
| 16:00 | 0.440 \pm 0.028 | 41.96 \pm 2.70 | 20.11 \pm 1.29 | 1.70 \pm 0.09 |
| 18:00 | 0.505 \pm 0.063 | 40.93 \pm 5.16 | 20.49 \pm 2.58 | 1.64 \pm 0.14 |

Conflict of Interest and Authorship Conformation Form

Peter Lindblad, corresponding author of the article entitled “CyanoFactory, a European consortium to develop technologies needed to advance cyanobacteria as photoautotrophic production chassis” and submitted to Algal Research journal, hereby declares:

- All authors have participated in (a) conception and design, or analysis and interpretation of the data; (b) drafting the article or revising it critically for important intellectual content; and (c) approval of the final version.
- This manuscript has not been submitted to, nor is under review at, another journal or other publishing venue.
- The authors have no affiliation with any organization with a direct or indirect financial interest in the subject matter discussed in the manuscript
- The following authors have affiliations with organizations with direct or indirect financial interest in the subject matter discussed in the manuscript:

Author's name and affiliation

Peter Lindblad ¹
Namita Khanna ¹
Adam Wegelius ¹

¹ Microbial chemistry, Department of Chemistry – Ångström, Uppsala University, Box 523, SE-751 20 Uppsala, Sweden

Röbbe Wünschiers ²
Gabriel Kind ²

² Biotechnology and Chemistry, University of Applied Sciences, Technikumplatz 17, DE-09648 Mittweida, Germany

Paula Tamagnini ^{3,4,5}
Catarina C. Pacheco ^{3,4}
Filipe Pinto ^{3,4}
Eunice A. Ferreira ^{3,4,6}
José Pereira ^{3,4}
Paulo Oliveira ^{3,4}

³ i3S – Instituto de Investigação e Inovação em Saúde, Universidade do Porto, Portugal

⁴ IBMC- Instituto de Biologia Molecular e Celular, Universidade do Porto, Portugal

⁵ Faculdade de Ciências, Departamento de Biologia, Universidade do Porto, Portugal

⁶ ICBAS - Instituto de Ciências Biomédicas Abel Salazar, Universidade do Porto, Portugal

Matthias Rögner ⁷
Sascha Rexroth ⁷
Joseph Keller ⁷
Katrin Wiegand ⁷

⁷ Plant Biochemistry, Faculty of Biology & Biotechnology, Ruhr University Bochum, D-44780 Bochum, Germany

Marko Dolinar ⁸
Helena Čelešnik ⁸

⁸ University of Ljubljana, Faculty of Chemistry and Chemical Technology, University of Ljubljana, Večna pot 113, SI-1000 Ljubljana, Slovenia

Andrew Landels ^{9,10}
Jennifer L Parker ⁹
Narciso Couto ⁹
T Khoa Pham ⁹
Josselin Noirel ¹²
Caroline Evans ⁹
Phillip C Wright ^{9,11}

⁹ ChELSI Institute, Department of Chemical and Biological Engineering, The University of Sheffield, Sheffield, UK

¹⁰ Plymouth Marine Laboratory, Prospect place, Plymouth, PL1 3DH, UK

¹¹ School of Chemical Engineering and Advanced Materials, c/- Faculty Office, Faculty of Science, Agriculture and Engineering, Newcastle University, Newcastle, NE1 7RU, UK

¹² Chaire de Bioinformatique, LGBA, Conservatoire National Des Arts Et Métiers, 75003 Paris, France

Javier F. Urchueguía ¹³
Maria Siurana ¹⁴
David Fuente ¹³
J. Alberto Conejero ¹⁴
Lenin Lemus ¹³

¹³ Instituto de Aplicaciones de las Tecnologías de la Información y de las Comunicaciones Avanzadas, Universitat Politècnica de València, Spain

¹⁴ Instituto Universitario de Matemática Pura y Aplicada, Universitat Politècnica de València, Spain

Hans-Jürgen Schmitz ¹⁵
Sarah Ocklenburg ¹⁵
Friederike Borbe ¹⁵
Mathias Wutschel ¹⁵

¹⁵ KSD Innovation GmbH, Germany

Giuseppe Torzillo ¹⁶
Eleferios Touloupakis ¹⁶
Bernardo Cicchi ¹⁶
Ana Margarita Silva Benavides ^{16,17}

¹⁶ Istituto per lo Studio degli Ecosistemi (ISE), Consiglio Nazionale delle Ricerche (CNR)
via Madonna del Piano, 10, I-50019, Sesto Fiorentino, Italy

¹⁷ Escuela de Biología & Centro de Investigación en Ciencias del Mar y Limnología
(CIMAR), Universidad de Costa Rica, San Pedro, San José 11501, Costa Rica

Marcello M. Diano ¹⁸
Serena Esposito ¹⁸

¹⁸ M₂M Engineering sas (M2M), Via Cinthia P.co S. Paolo, 13 Naples, Italy

Peter Lindblad (peter.lindblad@kemi.uu.se) takes responsibility for the integrity of the work as a whole, from inception to finished article.